

A NEW ELASMOSAURID (SAUROPTERYGIA: PLESIOSAURIA) FROM THE
BEARPAW FORMATION (LATE CRETACEOUS, MAASTRICHTIAN) OF MONTANA
AND THE EVOLUTION OF NECK LENGTH IN ELASMOSAURIDAE

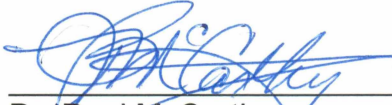
By

Danielle J. Serratos

RECOMMENDED:




Dr. Sarah Fowell



Dr. Paul McCarthy



Dr. Patrick Druckenmiller
Advisory Committee Chair

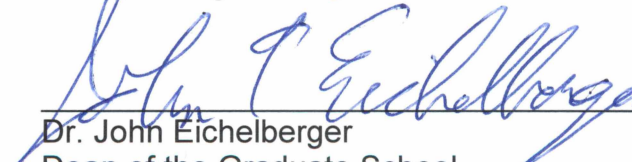


Dr. Sarah Fowell
Chair, Department of Geosciences


APPROVED:



Dr. Paul Lauer
Dean, College of Natural Science and Mathematics



Dr. John Eichelberger
Dean of the Graduate School



Date

A NEW ELASMOSAURID (SAUROPTERYGIA: PLESIOSAURIA) FROM THE
BEARPAW FORMATION (LATE CRETACEOUS, MAASTRICHTIAN) OF MONTANA
AND THE EVOLUTION OF NECK LENGTH IN ELASMOSAURIDAE

A
THESIS

Presented to the Faculty
of the University of Alaska Fairbanks

in Partial Fulfillment of the Requirements
for the Degree of

MASTER OF SCIENCE

By

Danielle J. Serratos, B.S.

Fairbanks, AK

August 2015

ABSTRACT

Plesiosauria is a diverse clade of marine reptiles that have been studied since the early 19th century. However, phylogenetic relationships within the group have been contentious due to limited taxon sampling and a misunderstanding of how ontogeny, interspecific and intraspecific variation affect character states. This is particularly true for elasmosaurids, a clade of long-necked plesiosaurians known from the Cretaceous. In 2010, a new, nearly complete skeleton, MOR 3072, was collected from the Late Cretaceous (Campanian-Maastrichtian) Bearpaw Shale of northeast Montana, and it provides morphological information rarely observed within Elasmosauridae. MOR 3072 consists of a complete skull, the anterior 23 cervical vertebrae, a partial dorsal and caudal vertebral column, incomplete pectoral and pelvic girdles, elements of both fore- and hindlimbs, ribs, and gastralia. Here, I present a detailed description of the specimen and conduct the most complete phylogenetic analysis of Elasmosauridae to date. A new taxon is recognized on the basis of the following suite of autapomorphies and unique character combinations: a chordate bilobed external naris, a squared-off posteroventral margin of maxilla, the presence of a maxilla-squamosal contact, a deep anteroposterior-oriented cleft in the articular posterior to the glenoid, a reduced number of cervical vertebrae, proximal caudal vertebrae that are wider than dorsoventrally tall, and small facets for forelimb and hindlimb preaxial accessory ossicles. A phylogenetic analysis places MOR 3072 as the sister taxon to the long-necked, Western Interior elasmosaurids *Hydralmosaurus serpentinus* + *Styxosaurus snowii*. Being early Maastrichtian in age, MOR 3072 is the stratigraphically youngest elasmosaurid yet known from the Western Interior Seaway. It is also one of the smallest adult

elasmosaurids ever recovered (4.5–5 m) and exhibits a reduced neck length due to a reduction in both the number of cervical vertebrae and centrum length, which is convergent with another clade of Maastrichtian elasmosaurids, *Aristonectinae*.

This thesis is dedicated to every girl who wants to be a scientist.

Table of Contents

	Page
Signature Page	i
Title Page	iii
Abstract	v
Dedication Page.....	vii
Table of Contents	ix
List of Figures	xi
List of Tables	xii
List of Other Materials	xii
Acknowledgements	xiii
General Introduction	1
Literature Cited	4
Thesis	7
Introduction	7
Geologic Setting	10
Methods	12

	Page
Systematic Paleontology	13
Description	15
Phylogenetic Analysis	39
Discussion	42
Figures	47
Tables	62
Literature Cited	66
Other Materials	74
General Conclusion	77
Literature Cited	80
Appendix	83

List of Figures

	Page
FIGURE 1. Map of locality	47
FIGURE 2. Articulated specimen with photo of MOR 3072	48
FIGURE 3. Dorsal view of skull	49
FIGURE 4. Ventral view of skull	50
FIGURE 5. Palatal view of skull	51
FIGURE 6. Hyoids	52
FIGURE 7. Atlas-axis	53
FIGURE 8. Cervical vertebrae 4, 8, and 18	54
FIGURE 9. Dorsal vertebrae	55
FIGURE 10. Caudal vertebrae and phalanges	56
FIGURE 11. Coracoid	57
FIGURE 12. Right forelimb	58
FIGURE 13. Ilium	59
FIGURE 14. Left hindlimb	60
FIGURE 15. Cladogram	61

FIGURE 16. Mean VLI of 13 elasmosaurid cervical series62

List of Tables

	Page
TABLE 1. Measurements	63
TABLE 2. Vertebral dimensions and VLI	65

List of Other Materials

	Page
O. M. 1. Character matrix scores of MOR 3072	74
O. M. 2. Strict Consensus tree	75
O. M. 3. Taxon Instability scattergram	76

ACKNOWLEDGEMENTS

First and foremost, thanks to Patrick Druckenmiller, Ph.D. and Roger Benson, Ph.D. Also a huge thanks to Mark Leckie, Ph.D. for his assistance in analyzing and understanding the paleoenvironment of the WIS. My sincere thanks go out to the volunteers that helped excavate the elasmosaur, the staff at the Charles M. Russell National Wildlife Refuge, and Beverly Skinner for making this excavation a priority in their busy lives. I would also like to thank Lynden Transport and UPS for shipping the specimen from Montana to Alaska. I am indebted to David Bradt and family—without finding the specimen in the first place, none of this would have been possible. Thanks as well to Joshua Slattery, Ph.D. and Neil Landman, Ph.D. for help identifying invertebrates within the matrix; Maciej Sliwinski, Ph.D. and Ken Severin, Ph.D. for the XRF scan and Barium analysis; the Fairbanks Memorial Hospital for allowing us to CT scan the skull; Jesse Pruitt and the Idaho Visualization Laboratory for the laser scans and 3D reconstruction; Elisabeth Nadin, Ph.D. for reviewing this paper; and Laurel Gangloff and Hannah Foss for help with figures. Special thanks go to my committee members, Paul McCarthy, Ph.D. and Sarah Fowell, Ph.D. A big thank you to everyone who helped prepare the specimen: Jacob Van Veldhuizen M.S., Alex Edgar, Emma Boone, Julie Rousseau M.S., and Meghan Shay! Thanks to dad, mom, and Courtney for their support and Judy Nayer for her book! Finally, I'd like to thank mi amor, Carlos, for bottomless love and much-needed laughter.

GENERAL INTRODUCTION

Plesiosauroians have been a source of much mystery and speculation throughout history because of their unusual body types, which are unlike anything alive today. One of the important early discoveries of this group was made by Mary Anning, an amateur fossil hunter from Lyme Regis, England, who found the first complete and articulated specimen of *Plesiosaurus* in 1823. Some of the best known examples of plesiosauroians in popular and scientific lore include the epic battle between a plesiosauroian and an ichthyosauroian in Jules Verne's 1864 classic, "Journey to the Center of the Earth" and the faked 'surgeon's photograph', made in 1934, of a mythical monster that still has people searching for a plesiosauroid in Loch Ness today. Edward Drinker Cope, a famed paleontologist, was so bewildered by the extreme neck length of *Elasmosaurus* (72 neck vertebrae in total) that he infamously published a description with the skull attached to the end of the tail because of his confusion in distinguishing cervical (neck) from caudal (tail) vertebrae.

Plesiosauroia (Sauropterygia) is a monophyletic clade of Mesozoic marine reptiles (Massare, 1987; Storrs, 1991). The group existed from the earliest Jurassic to the end of the Cretaceous and had a global distribution in open marine and nearshore settings (O'Keefe, 2001; Rieppel, 1998). These apex predators had a varied diet, including fish, other marine reptiles, cephalopods, bivalves, and gastropods (Massare, 1987; Buchy, 2005; McHenry et. al., 2005).

Two major end-member morphotypes exist in Plesiosauria: the short-necked and large-headed pliosaenomorphs, and the long-necked and small-headed plesiosaenomorphs such as elasmosaurids, which are the topic of this thesis. Plesiosaurians have traditionally been classified based upon the number of cervical vertebrae they possess, which ranges from *Brancaesaurus*, which only had 13 cervical vertebrae (Williston, 1903), to *Albertonectes*, which has 76 cervicals – the greatest number of neck vertebrae of any vertebrate known (Kubo et al., 2012). Plesiosaurians have been said to resemble turtles with no carapace and long necks, in part because of the shield-like gastralia that protect the ventral surface of their torso. Plesiosaurians also share fin-shaped frontlimbs and hindlimbs that are hyperphalangic (having extra phalanges = finger bones) but not hyperdactylous (having extra digits). The reduction of connectivity between the vertebral column and pelvic girdle via the ilia suggests that these animals could not support their own body weight on land and therefore reproduced at sea (O’Keefe and Chiappe, 2011). Another common element found in plesiosaurians are gastroliths, or rounded stones that might have been used to aid in digestion, help control buoyancy, or both.

Elasmosaurids (Elasmosauridae) are Cretaceous long-necked plesiosaurians that typically have more than 40 cervical vertebrae and a small head relative to body size. The diversity, anatomy, and relationships of elasmosaurids are still poorly understood despite an abundance of material found at a number of sites worldwide, particularly within the Cretaceous Western Interior Seaway (WIS) of North America. Unfortunately, elasmosaurids from the Western Interior are often poorly preserved or incomplete, making phylogenetic relationships within the clade difficult to determine.

The Western Interior Seaway (WIS) was an epeiric sea located in the Western Interior Basin (WIB) of North America which underwent numerous transgressive-regressive marine cycles throughout most of the Late Cretaceous (Kauffman et al., 1993). The Bearpaw Formation, in which the elasmosaurid described herein was found, is an upper unit of the Montana Group and consists of dark clay shales with numerous calcareous concretions. The Bearpaw Formation was deposited during the Campanian and Maastrichtian (latest Cretaceous) and records the last major transgressive-regressive cycle of the WIS (Kauffman et al., 1993). Thus, elasmosaurids from the Bearpaw are among the youngest members of the clade known from the WIB.

Character selection and definition of character states for use in establishing evolutionary relationships in Plesiosauria has developed slowly and often been contentious (Welles 1943; Storrs, 1993; O'Keefe 2001; Druckenmiller and Russell, 2008; Benson and Druckenmiller, 2013), especially those characters focused on neck length and cervical vertebral dimensions (O'Keefe and Hiller, 2006). While cladistic analyses of plesiosaurians have only been conducted in the last 15 years (O'Keefe, 2001; Sato, 2002; Druckenmiller and Russell, 2008; Ketchum and Benson, 2010), recent work by Benson and Druckenmiller (2013) has brought better resolution to the group as a whole by adding numerous specimens and characters to their matrix. While great strides have been made to establish stable relationships within Plesiosauria, the now well-established monophyletic clade Elasmosauridae is still one of the least resolved groups due to incomplete taxon sampling, poor understanding of anatomy, and a lack of agreement amongst researchers on character scores for phylogenetic analysis.

During the summer of 2010, elk hunter David Bradt found a nearly complete skeleton of an elasmosaurid in a deep ravine within the Charles M. Russell National Wildlife Refuge (CMRNWR) in northeastern Montana, U.S.A. (Fig. 1). The specimen, MOR (Museum of the Rockies) 3072 was found in the fall of 2010; however, a heavy spring runoff prior to excavation in July 2011 removed some of the exposed elements. At the time it was collected by Dr. Patrick Druckenmiller and a team of volunteers from the CMRNWR, the fossil lacked the posterior 16–19 cervical vertebrae (see Fig. 2 for photographic evidence of missing vertebrae), scapulae, clavicular arch, anterior portion of the coracoids, and distal limb and caudal elements.

Herein, I present a description and phylogenetic analysis of a new elasmosaurid plesiosaurian, unique among elasmosaurids for its remarkably short neck, both in terms of cervical vertebral count and proportions, and numerous other characters of the skull and postcranium. MOR 3072 represents the third elasmosaurid taxon described from the Bearpaw Formation and is one of the last plesiosaurians known from in the Western Interior Seaway. Finally, it provides important new morphological data for use in phylogenetic analyses of this clade and provides insight into the evolution and convergence of neck lengths within Elasmosauridae.

LITERATURE CITED

Benson, R.B.J., and P.S. Druckenmiller. 2013. Faunal turnover of marine tetrapods during the Jurassic–Cretaceous transition. *Biological Reviews* 1–23.

- Buchy, M. –C. 2005. An elasmosaur (Reptilia: Sauropterygia) from the Turonian (Upper Cretaceous) of Morocco. *Carolinea* 63:5–28.
- Druckenmiller, P. S., and A. P. Russell. 2008. A phylogeny of Plesiosauria (Sauropterygia) and its bearing on the systematic status of *Leptocleidus* Andrews, 1922. *Zootaxa* 1863:1–120.
- Kauffman, E. G., B. B. Sageman, J. I. Kirkland, W. P. Elder, P. J. Harries, and T. Villamil. 1993. Molluscan biostratigraphy of the Cretaceous Western Interior Basin, North America. *Geological Association of Canada Special Papers* 39:397–434.
- Ketchum, H. F., and R. B. J. Benson. 2010. Global interrelationships of Plesiosauria (Reptilia, Sauropterygia) and the pivotal role of taxon sampling in determining the outcome of phylogenetic analysis. *Biological Reviews* 85:361–392.
- Kubo, T., M. T. Mitchell, and D. M. Henderson. 2012. *Albertonectes vanderveldei*, a new elasmosaur (Reptilia, Sauropterygia) from the Upper Cretaceous of Alberta. *Journal of Vertebrate Paleontology* 32(3):557–572.
- Massare, J. A. 1987. Tooth morphology and prey preference of Mesozoic marine reptiles. *Journal of Vertebrate Paleontology* 7(2):121–137.
- McHenry, C. R., A. G. Cook, and S. Wroe. 2005. Bottom-feeding plesiosaurs. *Science* 310(5745):75.
- O’Keefe, F. R. 2001. The evolution of plesiosaur and pliosaur morphotypes in the Plesiosauria (Reptilia: Sauropterygia). *Paleobiology* 28(1):101–112.

- O'Keefe, F. R., and N. Hiller. 2006. Morphologic and ontogenetic patterns in elasmosaur neck length, with comments on the taxonomic utility of neck length variables. *Paludicola* 5(4):206–229.
- O'Keefe, F. R., and L. M. Chiappe. 2011. Viviparity and K-selected life history in a Mesozoic Marine Plesiosaur (Reptilia: Sauropterygia). *Science* 333(6044):870–873.
- Rieppel, O. 1998. The status of the Sauropterygian reptile genera *Ceresiosaurus*, *Lariosaurus*, and *Silvestrosaurus* from the middle Triassic of Europe. *Fieldiana Geology, New Series* 38:1–46.
- Sato, T. 2002. *Terminonatator ponteixensis*, a new elasmosaur (Reptilia; Sauropterygia) from the Upper Cretaceous of Saskatchewan. PhD Thesis, University of Calgary 1–412.
- Storrs, G. W. 1991. Anatomy and relationships of *Corosaurus alcovensis* (Diapsida: Sauropterygia) and the Triassic Alcova Limestone of Wyoming. *Peabody Museum of Natural History Bulletin* 44:1–163.
- Storrs, G. W. 1993. Function and phylogeny in Sauropterygian (Diapsida) evolution. *Functional Morphology and Evolution, American Journal of Science*, 293(A):63–90.
- Welles, S. P. 1943. Elasmosaurid plesiosaurs, with description of new material from California and Colorado. *University of California Memoirs* 13:125–254.
- Williston, S. W. 1903. North American plesiosaurs. *Field Columbian Museum, Publishing, Geological Series* 2(1):1–79.

THESIS

A NEW ELASMOSAURID (SAUROPTERYGIA: PLESIOSAURIA) FROM THE BEARPAW FORMATION (LATE CRETACEOUS, MAASTRICHTIAN) OF MONTANA AND THE EVOLUTION OF NECK LENGTH IN ELASMOSAURIDAE¹

INTRODUCTION

Plesiosauria is an extinct, monophyletic clade of secondarily aquatic Mesozoic marine reptiles. Plesiosaurians are fairly conserved with respect to their post-cervical body shape, but vary greatly in the relative proportions of skull size and neck length, ranging between two end-member morphotypes: the large-headed and short-necked pliosauromorphs and the small-headed and long-necked plesiosauromorphs (sensu O'Keefe and Carrano, 2005). Elasmosauridae is a derived clade of plesiosauromorph plesiosaurians that are diagnosed on having 40 or more cervical vertebrae (ranging to as many as 76), anterior cervical centra that exhibit lateral longitudinal ridges, cervical centra as long or longer than dorsoventrally tall, a constriction at the base of neural spines in dorsal vertebrae, elongate ilia, humeri that are proximodistally longer than femora, and humeri with a length versus width ratio of 2.2 or less (sensu Benson and Druckenmiller, 2013 and present study). Historically, a number of both Jurassic and Cretaceous plesiosauromorph genera have been included within Elasmosauridae (Carpenter, 1999; Gasparini et al., 2003; Großmann, 2007), but recent analyses restrict

¹ Serratos, D. J., P. S. Druckenmiller, and R. J. Benson. Prepared for submission to the Journal of Vertebrate Paleontology.

the clade to Cretaceous forms only (Sato, 2002; Kear, 2005; Ketchum and Benson, 2010; Benson and Druckenmiller, 2013). While the monophyly of Cretaceous Elasmosauridae is now well established, relationships within the clade are some of the least resolved among all plesiosaurians (Ketchum and Benson, 2010; Benson and Druckenmiller, 2013; Araújo et al., 2015a), in part due to a poor understanding of their cranial anatomy and incomplete sampling throughout their long fossil history, which spans nearly the entire Cretaceous. The lack of a well resolved phylogeny for the clade has resulted in a poor understanding of many issues regarding their evolutionary history, including the observed high degree of variation in neck length and their paleobiogeography.

Elasmosaurids are globally distributed, having been found in South America (Welles, 1962), Africa (Vincent et al., 2011; Lomax and Wahl, 2013), Australia (Kear 2005), New Zealand (Wiffen and Moisley, 1986; Cruickshank and Fordyce, 2002; Hiller et al., 2005), Asia (Sato et al., 2006) and Antarctica (O’Gorman et al., 2012). In North America, elasmosaurids are known from latest Cretaceous deposits along the west coast of California (Welles, 1943); however, the greatest diversity and actual number of specimens are found in Albian to Maastrichtian-aged deposits of the Cretaceous Western Interior Basin (WIB) (Welles, 1952; Carpenter, 1999). Based on current reviews, 9 monotypic genera of elasmosaurids are recognized in the WIB (Welles, 1943; Carpenter, 1999; Sato, 2003; Druckenmiller and Russell, 2006; Kubo et al., 2012), although it is likely actual species level diversity is greater still. Two genera from the Bearpaw Shale are the stratigraphically youngest-known forms from the WIB:

Terminonatator (Sato, 2003) and *Albertonectes* (Kubo et al., 2012). The latter possesses 76 cervical vertebrae, the greatest count known among all plesiosaurians.

In the fall of 2010, a new, nearly complete skeleton of an elasmosaurid was discovered in the Bearpaw Formation of Montana, U.S.A. The specimen, MOR 3072, was found fully articulated and in situ at the bottom of a narrow ravine within the C. M. Russell National Wildlife Refuge. At the time of discovery, much of the skeleton was preserved in a single large carbonate concretion, along with an articulated cervical series extending into the outcrop, which was carefully documented in a series of field photos by the discoverer (Fig. 2). Unfortunately, the posterior half of the neck and anterior portion of the concretion were lost to erosion the following spring due to an intense runoff event. At the time of excavation, the anterior half of the cervical series and a complete skull were collected from the surrounding outcrop, along with the uneroded portion of the postcranial skeleton, which contained the posterior two-thirds of the coracoids, an unknown number of dorsal vertebrae, ribs and gastralia, anterior caudal vertebrae, portions of the left and right fore- and hindlimbs, and much of the pelvic girdle (Fig 2).

MOR 3072 is significant in a number of respects. Stratigraphically, it is the youngest elasmosaurid described to date from the WIB and it possesses one of the shortest necks in terms of both cervical count and overall length of any elasmosaur known from North America. The quality of preservation in MOR 3072 also provides important new morphological data for elasmosaurids and permits the recognition of a new genus, described below. Finally, MOR 3072 is incorporated into a phylogenetic analysis using the largest existing phylogenetic data matrix of plesiosaurians, which

helps to resolve poorly understood relationships within Elasmosauridae and elucidates aspects of neck length evolution in the clade.

Institutional Abbreviations—**AMNH**, American Museum of Natural History, New York; **KUVP**, Natural History Museum, University of Kansas; **MOR** Museum of the Rockies, Bozeman, Montana; **RSM**, Royal Saskatchewan Museum, Regina, Saskatchewan, Canada; **SDSMT**, South Dakota School of Mines and Technology; **SMNK-PAL**, Staatliches Museum für Naturkunde Karlsruhe; **SMP-SMU**, Shuler Museum of Paleontology, Southern Methodist University, Dallas, Texas; **TMP**, Royal Tyrrell Museum of Paleontology, Drumheller, Alberta, Canada; **UAMES**, University of Alaska Museum Earth Sciences Collection, Fairbanks, Alaska.

GEOLOGIC SETTING

The Western Interior Basin (WIB) of North America records numerous transgressive-regressive marine cycles of the epicontinental Cretaceous Western Interior Seaway (WIS) (Kauffman et al., 1993). The WIS extended north-to-south across the North American continent, from the Gulf of Mexico to the Arctic Basin (He et al., 2005). The WIS had an estimated maximum depth of 200-500 m (Kauffman, 1984) and was present from the middle Cenomanian to late Maastrichtian (Cobban et al., 2006).

The Bearpaw Formation is an upper unit of the Montana Group and consists of dark clay shales with numerous calcareous concretions. The Bearpaw ranges between 60 m and 335 m thick (Cobban et. al., 2006; Feldmann, 2012) although the thickness at the discovery site of MOR 3072 was not measured. This westward-thinning tongue of

marine shale disconformably overlies the Judith River Formation and is conformably overlain by the Fox Hills Sandstone in Montana (Feldmann et al., 1977; Condon, 2000) and the Eastend Formation in Canada (He et al., 2005). The Bearpaw Formation grades eastward into the Pierre Shale (Condon, 2000) and the outcrop similarity between the Bearpaw and Pierre shales makes these two units physically synonymous in the upper midcontinent of North America (Tourtelot, 1962; Feldmann, 2012).

The paleoenvironment of the Bearpaw Sea has been reconstructed by numerous authors using a variety of methods. Dinoflagellates from the shale in central Montana suggest a low-salinity marine environment (Palamarczuk and Landman, 2011). This idea is further supported by freshwater algae associated with dinoflagellates (Palamarczuk and Landman, 2011; Cochran et al., 2003). The presence of diatoms may indicate a nutrient-rich and fertile Bearpaw Seaway (Bergstresser and Krebs, 1983). Paleotemperatures of the Bearpaw Sea have been estimated based on $\delta^{18}\text{O}$ and $\delta^{13}\text{C}$ values of molluscs to fluctuate between 12° and 19° C during the middle Maastrichtian (He et al., 2005).

Samples from the shale and concretion matrix surrounding MOR 3072 were analyzed for foraminifera and other carbonaceous material. The shale found around MOR 3072 is nearly pure mud with very little quartz and carbonaceous material. While no forams were found, pyritized diatoms and glauconite grains were found in both the shale and concretion matrix that encased the specimen (pers. comm. Mark Leckie) using a standard micropaleontological disaggregation method (Leckie et al., 1991). Pyritized diatoms are commonly found in Late Cretaceous WIB strata (Bergstresser and Krebs, 1983) and indicate a seaway with rich primary production. I infer that MOR 3072

died in a relatively shallow marine environment with low sedimentation rate due to the absence of deltaic input or steady and significant freshwater influx from nearby shorelines.

The Bearpaw Formation was deposited during the Campanian and Maastrichtian and records the last transgressive-regressive cycle of the Western Interior Seaway (Kauffman et al., 1993). The stratigraphic position of MOR 3072 within the Bearpaw was assessed on the basis of two ammonites recovered at the discovery site, which were identified as either *Baculites grandis* or *B. baculus* (pers. comm., Joshua Slattery and Neil Landman). *B. grandis* (70.00 ± 0.4 MYA) and *B. baculus* (70.4 ± 0.5 MYA) indicate an early Maastrichtian age (He et al., 2005; Larson and Landman, 2007), which correlates to the *Endocostea typical*, *Inoceramus incurvus* and *Trochoceras radiosus* Inoceramid Interval Zones of Cobban et al. (2006) and the Foraminiferal zone *Haplophragmoides excavate* (He et al., 2005). Thus, MOR 3072 is the youngest Western Interior elasmosaurid presently described, being younger than *Terminonatator* (Campanian *Baculites cuneatus*–*B. reesidei* zone) and *Albertonectes* (Campanian *B. compressus* zone) (Sato, 2003; Kubo et al., 2012).

METHODS

The skull and anterior half of the cervical series were preserved in a relatively soft shale, which was mechanically prepared using dental picks, air scribes, and air abrasive techniques. The preserved portion of the postcranial specimen was encased within a large carbonate concretion that was broken into smaller pieces in the field

before transport to UAMES for preparation. The concretionary block was both mechanically and chemically prepared using air scribes and repeated immersion in a 7% formic acid bath.

The skull of MOR 3072 was scanned using computed tomography (CT) at a medical facility; however, clear results were not obtained, likely due to high levels of elemental barium (approximately 10%) detected using X-ray fluorescence. The skull and anterior four cervical vertebrae were also scanned using a 3D laser. Two-dimensional TIFF files were developed through modification of these 3D files and implemented in figures 3 and 4 for a high-contrast visual of the skull.

SYSTEMATIC PALEONTOLOGY

DIAPSIDA Osborn, 1903

SAUROPTERYGIA Owen, 1860

PLESIOSAURIA De Blainville, 1835

XENOPSARIA Benson and Druckenmiller, 2013

ELASMOSAURIDAE Cope, 1869

gen. nov.

Type and Only Species—*gen. nov.*

Horizon—Bearpaw Formation, lower Maastrichtian, Upper Cretaceous.

Diagnosis—As for the type and only species *gen. nov.*

gen. et sp. nov.

Holotype and Only Specimen—MOR 3072 including the skull, articulated anterior 23 cervical vertebrae, dorsal and anterior caudal vertebrae, partial coracoids, much of the humerus, epipodial and mesopodial rows of the forelimb, both ilia and portions of the pubis and ischium, complete femur and portions of the epipodial row of the hind limb, and numerous ribs and gastralia.

Locality and Horizon—Near Fort Peck Reservoir, Phillips County, Montana within the Charles M. Russell National Wildlife Refuge. Precise coordinates of the discovery site are on file with the C. M. Russell National Wildlife Refuge office. Found in the *Baculites baculus*–*B. grandis* Zones of the Bearpaw Shale, lower Maastrichtian, Upper Cretaceous.

Diagnosis—MOR 3072 is an elasmosaurid plesiosaurian (sensu Benson and Druckenmiller, 2013) possessing the following autapomorphies: chordate bilobed external naris; squared-off posteroventral margin of maxilla; maxilla-squamosal contact; deep anteroposterior-oriented cleft in articular posterior to glenoid; proximal caudal vertebrae wider than dorsoventrally tall; and small articular facets for hindlimb preaxial accessory ossicles.

MOR 3072 can further be diagnosed on the following unique character combinations: relatively short rostrum, with rostral index of 33; absence of mandibular keel; dorsoventral oriented premaxilla-maxilla suture; postfrontal participation in both orbital and temporal margins; postorbital extends half the length of the ventral margin of the supratemporal fenestra; pineal slit level with postorbital bar; coronoid process made

of dentary only; weakly developed medial pterygoid processes that do not obscure basisphenoid/basioccipital; anteriorly inclined basioccipital ventral plate; 39–42 cervical vertebrae; absence of lateral longitudinal ridge of the cervical vertebrae; lateral expansion of intercoracoid vacuity; and dorsal expansion of ilia twice the anteroposterior width of the midshaft.

DESCRIPTION

General Comments

MOR 3072 was found in articulation with the ventral surface of the body stratigraphically up. Much of the postcranial skeleton occurs in one large carbonate concretion (1.2 m long, 1.0 m wide), while the skull and the proximal 23 cervical vertebrae were found in the surrounding soft shale (Figure 2). There are an estimated total of 39–42 cervical vertebrae, 16–19 of which were lost in a heavy spring runoff that occurred between the time of discovery and excavation. Elasmobranch teeth are found scattered throughout the concretionary block. Teleost scales are also found in both the shale and, less commonly, within the concretion. A layer of macerated invertebrate material is preserved under postcranial elements within the concretion. Barite crystals were scattered around the postcranium but concentrated near the coracoid and acetabulum. A thin encrusting layer of pyrite has been located on bones in both the shale and concretionary matrix.

Total body length of MOR 3072 is estimated at 4.5–5 m. This was achieved by adding the length of the skull, preserved cervical series, and length of the articulated

block (Fig. 2) to the estimated length of the missing portion of the posterior cervicals and anterior pectoral girdle using field photographs. Tail length for MOR 3072 was estimated based upon the percentage of tail to overall body length in *Albertonectes vanderveldei* and *Morenosaurus stocki*. MOR 3072 is considered an adult based upon the high degree of fusion of the atlas and axis, fusion of neurocentral sutures (although the sutures remain visible in some of the cervicals) and most cervical ribs, and the extent of ossification of limb elements (Brown, 1981).

Skull

The skull of MOR 3072 is complete but obliquely crushed laterally, with the mandible remaining articulated to the cranium (Fig. 2). The left side of the skull is the best preserved and the basis for most interpretations, unless otherwise noted (Fig. 3). Only a small dorsolateral portion of the left squamosal appears to have been lost. The right side of the skull provides a partial view of the palate (Fig. 4).

MOR 3072 has a very short rostrum compared to other North American elasmosaurids (Sato, 2003). The beak index (percentage of preorbital region compared to the total skull length; Welles, 1952) is 33 for MOR 3072, similar to *Terminonatator ponteixensis* (35) but much less than most elasmosaurids, which average 40 (Sato, 2003). This shortening results in a premaxilla-maxilla suture that is nearly vertically oriented compared to *Styxosaurus snowii* and *Libonectes morgani*, both of which have premaxilla-maxilla sutures that are inclined posteriorly. The supratemporal fenestra is 38% of the total skull length (Table 1), nearly identical to *L. morgani*, but the relative

orbit to skull length—17% in MOR 3072 and 22% in *L. morgani*—falls within the range of variation noted for elasmosaurids in general (Araújo and Polcyn, 2013).

Dorsal Elements of the Skull—The premaxilla-maxilla boundary, which is well sutured and difficult to discern, extends dorsally from the posterior margin of the fifth alveolus to the midpoint of the ventral margin of the ventral lobe of the external naris. The premaxilla forms the entire anterior and dorsal border of the external naris, which is uniquely shaped like an inverted heart and bears two lobes, one anteriorly projecting and one ventrally projecting lobe (Fig 3). This autapomorphic feature differs from the oval external nares seen in other elasmosaurids such as *Libonectes morgani* and *Hydrotherosaurus alexandrae*. Relative to overall skull size, the external naris is also conspicuously small compared to most elasmosaurids, with the exception of *Zarafasaura oceanis* (Vincent et al., 2011). The posteromedian processes of the premaxillae border the medial margins of the frontals, just anterior to a deeply interdigitating premaxilla-parietal suture. The premaxillae form a prominent and narrow dorsomedian ridge, which extends along their entire length and is most pronounced in the region dorsal to the external nares. However, the ridge does not appear to possess as sharp or prominent a mound or dorsomedian ‘bump’ as that seen in lateral view on *Styxosaurus snowii* (Sato, 2003). Numerous neurovascular foramina are located on the external surface of the premaxillae but the texture is generally smooth and lacks any prominent crests or ridges.

The left and right maxillae each bear 14 alveoli. In lateral view, the alveolar margin is slightly sigmoid in outline, with the anterior portion concave downward and the posterior portion convex, very similar to the alveolar margin of *Styxosaurus snowii*. The

maxilla does not appear to contact the margin of the external naris, but the absence of a clear maxilla-prefrontal suture makes this relationship difficult to determine (Fig. 3). Both the left and right maxillae are displaced along the ventral margin of the orbit at their contact with the jugal. Posteriorly, the maxilla narrows in dorsoventral height and terminates, along with the tooth row, ventral to the approximate midpoint of the temporal fenestra. The maxilla possess a small posteroventrally extending flange from the ventral margin of the temporal bar that bears a short contact with the squamosal, an autapomorphic feature of this species. In palatal view, the maxilla forms the lateral margin of the internal naris. Adjacent to the primary alveoli, the surface texture of the maxilla is highly pitted, similar to the 'strong rugosity' located near the posterior premaxillary teeth of *Zarafasaura oceanis* (WDC CMC-01; Lomax and Wahl, 2013) that completely obscures all of the maxilla-palatine contact. In MOR 3072 the internal nares lies just posterior to the external nares, which differs somewhat from *Libonectes morgani*, where the posterior half of the internal nares overlaps with the anterior half of the external nares.

The orbit is roughly triangular with an anteroventral lobate extension, but it is not extended to the same extent as that seen in the holotype of *Styxosaurus* (KUVP 1301). The prefrontal forms the ventral third of the anterior margin of the orbit. The prefrontal is interpreted to participate in the posterior margin of the external naris as is typical of elasmosaurids (Carpenter, 1997) although its sutural relationship to the maxilla is not discernable. The prefrontal shares a short contact with the premaxilla dorsal to the external naris. A well-defined interdigitating frontal-prefrontal suture is visible near the approximate midpoint of the orbital margin. The frontal forms approximately 60% of the

anterodorsal border of the orbital margin and contacts the premaxilla medially. Its lateral margin is slightly convex and projects posteroventrally into the orbit. On the left side, the frontal-postfrontal suture is interpreted to lie along a break between these two elements, where the postfrontal overlaps the frontal at the dorsal orbital margin. The interdigitating postfrontal-postorbital suture is also marked by a break near the posterodorsal margin of the orbit, a feature that is mirrored on both sides of the skull. The postfrontal participates in the margins of both the orbit and the supratemporal fenestra, unlike the condition seen in *Zarafasaura oceanis* (Vincent et al., 2011) and *Hydrotherosaurus alexandrae* (Welles, 1943), in which the postfrontal only participates in the margin of the temporal fenestra.

The postorbital forms the dorsal two-thirds of the posterior orbital margin. Anteriorly, the postorbital-jugal suture is visible at the orbital margin but is difficult to trace posteriorly where a change in bone-fiber orientation is the basis for delimiting the two bones. The posterolateral process of the postorbital is very long and forms approximately half of the anteroventral margin of the temporal fenestra and the entire dorsal border of the jugal, thereby excluding the jugal from participating in the margin of the temporal fenestra. The postorbital of *Kaiwhekea katiki* also participates in the margin of the orbit and temporal fenestra but differs from MOR 3072 in not continuing posteriorly to contact the squamosal, thus allowing the jugal to participate in the temporal fenestra margin. The jugal of MOR 3072 is broadly rectangular in shape with the anteroposterior axis longest. It forms the posteroventral margin of the orbit and is completely bordered ventrally by the maxilla. The jugal-squamosal suture is subvertical

and occurs near the midpoint of the temporal bar. A small number of prominent foramina are visible on the jugal, and to a lesser extent, on the postorbital.

The anterior margin of the parietal lies immediately dorsal to the apex of the orbit, similar to *Libonectes morgani*, whereas in *Zarafasaura oceanis* and *Callawayasaurus columbiensis* the parietal-premaxilla suture lies posterior to the dorsal apex of the orbit. A distinct pineal foramen is not present although a narrow slit located at the anterior end of the parietal crest, immediately dorsal to the postorbital bar, may represent a remnant of this structure. Immediately anterior to and surrounding the pineal slit, the surface texture of the parietal bears numerous, small, anteroposteriorly-oriented ridges, but the surface texture becomes smooth posteriorly along the parietal crest. In lateral view, the dorsal margin of the parietal crest of MOR 3072 rises abruptly dorsally at its anterior end but posteriorly it is oriented nearly horizontally. In contrast, the highest point of the parietal crest lies near the midpoint of the supratemporal fenestra in *Kaiwhekea katiki*, while in *Thalassomedon hanningtoni* and *Styxosaurus snowii* the dorsal margin of the crest becomes progressively taller posteriorly and reaches its greatest height near its contact with the squamosal. In both the holotype and referred specimens of *Z. oceanis* (OCP-DEK/GE 315 and WDC CMC-01, respectively) the posterodorsal third of the supratemporal fenestra and parietal crest is formed by the squamosal (Vincent et al., 2011; Lomax and Wahl, 2013), thus differing markedly from MOR 3072 where the entire crest is formed by the parietal.

The suspensorium of MOR 3072 is inclined anteriorly at 15° from vertical. The dorsal processes of the squamosal extend posterolaterally from the midline symphysis, which lies anterior to the occipital condyle, creating a V-shaped profile in dorsal view.

The squamosal symphysis is robust but does not project posteriorly to form a 'bulb' as seen in *Styxosaurus snowii*. In posterior view, the ventromedial process of the squamosal is slightly less than half of the length of the quadrate shaft. The quadrate-squamosal suture is visible laterally, posteriorly and medially due to the arching nature of the squamosal dorsal to the quadrate. The quadrate ramus of the pterygoid contacts the pterygoid ramus of the quadrate along a distinct suture that is anterodorsally inclined and located posterior to the occipital condyle. The anterior ramus of the squamosal is bordered anteriorly by the postorbital dorsally and the jugal and maxilla ventrally. The posterodorsal margin of the temporal bar is squared-off where the anterior ramus and dorsal ramus of the squamosal diverge.

Braincase—Portions of the epipterygoid, prootic, supraoccipital, exoccipital-opisthotic and basisphenoid can be seen in the left supratemporal fenestra (Fig 3). Elements of the lateral wall of the braincase are fused but their contacts can be clearly traced by changes in bone fiber orientation. The left prootic is dorsoventrally taller than anteroposteriorly long and contacts both the anterior margin of the exoccipital-opisthotic and the anteroventral margin of the supraoccipital. The supraoccipital is also dorsoventrally taller than anteroposteriorly wide. Due to crushing, the posterior surface of the supraoccipital is not visible, nor is the ventrolateral portion of the exoccipital-opisthotic; thus foramina for exits of the cranial nerves cannot be seen. The paraoccipital process is longer than the dorsoventral height of the exoccipital-opisthotic and is mediolaterally narrower than dorsoventrally tall. Any lateral curvature of the paraoccipital process that may have been present is lost due to crushing. The posterior end of the paraoccipital process broadly contacts the quadrate and the squamosal.

Because the pterygoid-quadrato suture is also clearly visible, there is a small but clear contact between the paraoccipital and pterygoid (Fig 4). *Libonectes morgani* has a proportionally longer pterygoid ramus of the quadrato-quadrato ramus of the pterygoid than MOR 3072, but the suture is not well marked, so it is unclear if the pterygoid of *L. morgani* contacts the paraoccipital process. The paraoccipital process is interpreted to have inclined ventrally relative to the ventral surface of the exoccipital-opisthotic prior to taphonomic deformation.

The basioccipital bears a prominent ventral plate that differs from other elasmosaurids by being anteriorly inclined, in contrast to the vertical orientation (Fig. 5) seen in *Libonectes morgani*. The ventral plate bears a weakly developed dorsoventral ridge along the midline, unlike the prominent keel and paired lateral concavities of *Libonectes morgani*. In ventral view, the occipital condyle lies anterior to the quadrato condyle. Posteriorly, the occipital condyle is dorsoventrally taller than mediolaterally wide (2.9 cm by 2.4 cm) and is sub-rounded. The occipital condyle lacks a notochordal pit.

Palate—The anteromedial margin of the palatine forms the posterior border of the internal naris. The palatine closely approaches the contact along its midline as well as the posterior margin of the vomer, but direct contact between these elements cannot be observed due to crushing. Posteriorly, the palatine can be seen bordering the anterior margin of the ectopterygoid, but deformation of the skull has obscured the anterolateral margin.

The anterior ramus of the pterygoid closely approaches and may contact the posterior margin of the vomer. The anterior interpterygoid vacuity is absent, similar to all

other known elasmosaurids. A prominent pterygoid boss is located along the anterior margin of the subtemporal fenestra, two-thirds of which is formed by the lateral ramus of the pterygoid and one-third by the ectopterygoid. The pterygoid boss projects approximately 1 cm ventrally from the palatal surface and is anteroposteriorly longer than wide (length: 2.6; width: 0.9 cm). Only the portion of this boss that is composed of the pterygoid is rugose along its ventral surface. Although somewhat flattened taphonomically, the ventral surfaces of the lateral rami of the pterygoids are anteroposteriorly 'dished', similar to *Callawayasaurus columbiensis* and *Libonectes morgani*. The medial processes of the pterygoids posterior to the posterior interpterygoid vacuity are weakly developed and appear to share only a small contact along the midline, a configuration unique among elasmosaurids (Figs. 4 and 5). In contrast, the medial processes of the pterygoids of *L. morgani*, *C. columbiensis*, and *Zarafasaura oceanis* (Vincent et al., 2011) meet along the midline in a broad zone leaving a small portion of the basicranium visible. MOR 3072 lacks a pterygoid lappet, which is present in *L. morgani* (O'Keefe, 2001) and *C. columbiensis* (Appendix 2, Benson and Druckenmiller, 2013).

The pterygoids are split medially by the cultriform process of the parasphenoid at the anterior end of the posterior interpterygoid vacuity. The ventral surface of the cultriform process is flat anteriorly but then develops a narrow median keel posteriorly along most of the length of the interpterygoid vacuity. A posteriorly-oriented process, approximately 7 mm long, projects from the ventral margin of the parasphenoid keel. This parasphenoid process is similar in shape to that of *Libonectes morgani* but is positioned more anteriorly than it is in *L. morgani*. The midpoint of the posterior

interpterygoid vacuity is coplanar with the anterior margin of the subtemporal fossa. Within the posterior interpterygoid vacuity the parasphenoid underlaps the basisphenoid; posteriorly it may also underlap part of the basioccipital just anterior to the medial processes of the pterygoids, although the exact location of the element is equivocal.

Mandible—There are 19 alveoli in the left dentary, 18 in the right, and three alveoli adjacent to the mandibular symphysis. There is a conspicuous absence of a symphyseal keel on the ventral surface of the mandible, unlike SDSMT 451 and *Thalassomedon haningtoni*. The symphyseal region is pitted in a manner consistent with that of the premaxillae. In lateral view, the dentary varies in dorsoventral height due to a slight sigmoid curvature of the tooth row. Laterally, the dentary extends 69% of the length of the entire mandibular ramus. The extent of bowing of the mandibular ramus is not possible to determine due to taphonomic distortion. The left coronoid process (=eminence) is not visible laterally, but the posterior margin of the right process can be seen ventral to the supratemporal fenestra. Here, the coronoid process rises nearly vertically from the surangular-dentary contact, which lies along the posterior margin of the process. Thus, the coronoid process is formed entirely by the dentary, similar to that seen in *Styxosaurus snowii* but differing from *Libonectes morgani*, where the surangular and dentary contribute equally. In MOR 3072, the anterior margin of the coronoid process is not visible, but the posterior margin is concave and the overall shape appears very similar to the triangular morphology seen in *Terminonatator ponteixensis*.

In lateral view, the posterior margin of the dentary is formed along a subvertical suture that lacks a prominent posterior projection into the surangular-angular contact,

similar to that of *Libonectes morgani*. The surangular contacts the angular along a straight suture just ventral to the ventral margin of the mandibular fossa. The anterodorsal surface of the retroarticular process bears a deep cleft that lies immediately posterior to the mandibular fossa. The retroarticular processes of *Thalassomedon haningtoni* and *Styxosaurus snowii* display a similar shape, curvature and orientation to those of MOR 3072 but lack the deep fossa. *Callawayasaurus columbiensis* and *Terminonatator ponteixensis* have reduced retroarticular processes without a fossa. The retroarticular process of MOR 3072 is anteroposteriorly longer than the mandibular fossa and is dorsoventrally taller than wide in cross section, being mediolaterally widest in its dorsal half. The dorsoventral orientation of the retroarticular process is nearly horizontal and is slightly deflected medially in dorsal view. The posterior end of the retroarticular process is concave.

Elements of the medial surface of the mandible are best exposed on the left ramus (Fig 4). The anterior margin of the splenial participates in the mandibular symphysis, but the angular does not. The splenial is bordered ventrally by the angular in the region between the 6th to the 13th alveoli and posteriorly by the prearticular. The splenial terminates at the anterodorsal edge of the opening for the Meckelian canal. The angular-prearticular contact extends horizontally from the 14th alveolus to a zone of slightly rugose bone ventral to the mandibular fossa. The angular-prearticular suture is not tightly fused along its entire length; rather it is separated by two slit-like foramina. The opening for the Meckelian canal is an elongate (50 cm), slit-like structure inclined at approximately 25 degrees from the horizontal. The Meckelian canal is bordered

ventromedially by the prearticular, dorsally by the surangular, and posteriorly by the articular just anterior to the mandibular fossa.

Hyoids—Both hyoids were recovered from the palate of the skull (Fig. 6). The right hyoid was discovered encased in shale matrix at the posterior end of the skull, ventral to medial processes of the pterygoid. The left hyoid was located ventral to the palatine, which suggests slight taphonomic displacement. The hyoids have concavities at both the anterior and posterior surfaces, the anterior of which is larger in diameter. An anteroposteriorly-oriented channel is depressed along the length of the shaft beginning and ending approximately 1 cm before the anterior and posterior margins. The midshaft rises dorsally in medial view but the entire structures are straight in dorsal view. A review of the elasmosaurid literature reveals that hyoids are very rarely preserved and have only been found in *Eromangasaurus* (Kear, 2005), QMF 11050 (= '*Tuarangisaurus*' *australis*) (Sachs, 2005), and *Aristonectes quirquinensis* (Otero et al., 2014).

Dentition—The teeth of MOR 3072 are curved both distally and lingually. Most teeth are also gently inclined anteriorly. Tooth size varies dramatically along the toothrow. The anterior teeth are relatively small, but the first premaxillary tooth is not significantly smaller than the third, unlike *Terminonatator ponteixensis* where the first premaxillary tooth is much smaller than any other premaxillary teeth (Sato, 2003). The largest caniniform teeth are located posteriorly in the premaxilla and anteriorly in the maxilla. In the posterior half of the toothrow, the dentary teeth are consistently larger than their corresponding maxillary teeth. Teeth of the upper and lower toothrows generally display an interdigitating relationship with one another, with the exception of two pairs of adjacent teeth (the third and fourth left maxillary teeth and the eighth and

ninth right maxillary teeth) that lack a gap to accommodate an intervening dentary tooth. A similar relationship is seen in some tooth positions of *Callawayasaurus columbiensis* and *Libonectes morgani*.

The teeth of MOR 3072 are D-shaped in cross-section at the base of the crowns, with the labial surface being flat. There are enameled ridges concentrated on the medial, lingual and distal surfaces of both upper and lower crowns, though none are observed on the labial surface. Some ridges extend straight from the base to the midpoint of the crown and converge or terminate apically, while other ridges occur only at the base. Significant wear facets are seen on the eighth and ninth left maxillary teeth as well as the ninth right maxillary tooth and the eighth dentary tooth.

Axial Skeleton

The collected portion of the cervical series includes 23 vertebrae, all but one of which (number 23) were found in articulation. The total number of missing cervicals in MOR 3072 (excluding pectorals) was estimated based upon data gleaned from multiple photographs of the complete skeleton taken at the time of discovery. 15 additional vertebrae can be clearly counted in the field photographs, all of which have ventrally-positioned, sub-circular rib facets. The number of remaining cervicals that are wholly contained within the concretion are estimated by extrapolation from the last clearly visible vertebra (38) to the approximate anterior edge of the pectoral girdle, the location of which was determined by the placement of the coracoids following preparation. I estimated that the first pectoral vertebra would be dorsal to the anterior half of the scapulae based upon articulated skeletons of *Albertonectes vanderveldei*,

Hydrotherosaurus alexandrae, and *Morenosaurus stocki* (Welles, 1943). One or two vertebrae seen emerging from the cliff may also have been lost to erosion. Hence, I estimated as few as 39 to as many as 42 cervical vertebrae in total. Absolute neck length is estimated at 2.2 m (excluding skull) based upon comparisons of the posterior preserved cervical vertebrae, pectoral girdle, and forelimb elements to photographs of the complete skeleton. Thus, MOR 3072 has both the fewest total number of cervical vertebrae of any known North American elasmosaurid and the shortest adult neck in terms of relative and absolute length (see Discussion below).

Atlas-Axis Complex—Sutures of the atlas-axis complex are fused except those of the axial neural arch. As is typical for elasmosaurids, the atlantal centrum does not participate in the anterior margin of the atlantal cup, being excluded by the atlantal neural arch (Fig. 7). In anterior view, the atlantal centrum is visible and deeply recessed within the atlantal cup, but not visible laterally. In lateral view, a small opening (described as a ‘pit’ by Kubo et al. [2012] for *Albertonectes vanderveldei*) is situated between the base of the atlantal and axial neural spines, which are fused dorsally. Ventrally, the atlas-axis has a prominent hypophyseal ridge that originates on the anterior half of the atlantal centrum and extends posteriorly along most of the length of the axial centrum. Ventral to the atlas, the ridge is mediolaterally broad and flat ventrally but becomes sharply keeled ventral to the axis. The neural spine slopes posterodorsally at approximately 25–30 degrees, similar to *Libonectes morgani*, *Thalassomedon haningtoni*, and *A. vanderveldei*. Both the atlas and axis possess distinct ribs that are separate proximally but fuse distally (Fig. 7). The atlantal ribs extend posterior to the posterior margin of the axis centrum.

Postaxial Cervical Series—All of the collected cervical centra are mediolaterally wider than anteroposteriorly long (as measured along the posterior face) and dorsoventrally taller than long (Table 2, Fig. 8). Based upon field photographs, the posterior cervical vertebrae are also mediolaterally wider than anteroposteriorly long, although the relative dorsoventral height is difficult to determine. The anteroposteriorly short cervicals differ markedly in proportions from the anterior to middle cervicals of *Styxosaurus snowii*, *Albertonectes vanderveldei* and *Elasmosaurus platyurus* (Sachs, 2005). The Vertebral Length Index (VLI, see Discussion) for cervical vertebrae 3–23 range from 74.7-99.7 (mean = 90.8). By comparison, other Western Interior elasmosaurids such as *Thalassomedon haningtoni*, *Libonectes morgani*, *Hydralmosaurus serpentinus*, *Styxosaurus snowii*, *Terminonatator ponteixensis*, SDSMT 451, and *E. platyurus* have mean VLIs of 103-138.

In posterior view, a weakly developed ventral notch is present in the third cervical which becomes increasingly better developed and more conspicuous by vertebra nine. Centra 10–23 are clearly binocular-shaped due to the presence of a prominent ventral notch. In posterior view, as seen in photographs, the posterior cervicals have broad ventral notches that diminish in size posteriorly along the series. All preserved cervicals have a shallow groove that parallels the perimeter of the articular surfaces of the centra, similar to *Hydrotherosaurus alexandrae* and *T. ponteixensis*. The prominence of this feature in MOR 3072, which is clearly an adult, suggests it is not solely a juvenile characteristic (Brown, 1981; Ketchum and Benson, 2010; Benson and Bowdler, 2014).

Unlike most North American elasmosaurids, MOR 3072 lacks a lateral longitudinal ridge on all preserved cervicals, similar to the aristonectine *Kaiwhekea katiki* and

Futabasaurus suzukii. A rugosity is present along the lateral articular surfaces of the centra, immediately anterior and posterior to the rib facets, beginning at cervical nine. Posteriorly, the rugosity becomes more pronounced and expands dorsally along the articular rims; this is clearly visible in field photographs of posterior cervicals. Anterior cervical rib facets are subcircular but become slightly anteroposteriorly longer throughout the preserved series beginning at cervical 20. Anterior rib facets are situated slightly posteriorly on the centra, but shift to a more central position in posterior cervicals. *Morenosaurus stocki* similarly retains subcircular rib facets throughout its cervical series, unlike the middle to posterior cervicals of *S. snowii* and *A. vanderveldei* that have distinctly anteroposteriorly elongate facets. A narrow ventral median keel is present in vertebrae 3–7 and becomes a well-developed, mediolaterally broad and rounded ventral ridge in more posterior centra. A ventral ridge is also visible in vertebrae from the posterior half of the cervical series, although it is difficult to determine if the ridges were rounded or flat from photographs. Diminutive (2–5 mm long) paired subcentral foramina are present in all cervicals.

The neural arches are firmly fused to centra throughout the entire preserved series but the neurocentral sutures remain clearly visible. Neural arch facets are rectangular and extend almost the length of the dorsal surface of the centra unlike TTU P 9219 (Chatterjee and Small, 1989), which has smaller, oval shaped facets. Dimensions of the neural arches and spines from the missing posterior cervicals are unknown. The left and right pre- and postzygapophyses are all fused along the midline; however, they do not fuse along their entire length so that in dorsal view the anterior margins of prezygapophyses (and posterior margin of postzygapophyses) are U-shaped in outline,

similar to *A. vanderveldei* (Fig. 8). Each prezygapophyseal facet is concave, with the fused left and right facets producing a U-shaped trough in anterior view.

Postzygapophyseal facets are similarly convex. Numerous tiny pits are clustered on the anteroventral surface of prezygapophyses and on the posterior surface of neural arches ventral to the postzygapophyses. Neural spines of the anterior 23 cervical vertebrae are shifted posteriorly, such that the anterior margins of neural spines are collinear with the midpoint of their respective centra. In lateral view, the dorsal margins of neural spines slope anteriorly at approximately 10 degrees, and the anterior margins of neural spines are concave. In *Zarafasaura oceanis* (Lomax and Wahl, 2013) and *Libonectes atlasense* (Buchy, 2005) the cervical neural spines also slope anteriorly but at a much steeper angle (~45 degrees). In lateral view, the third and fourth neural spines are taller than long, cervical spines 5–9 are approximately equidimensional, and spines 11–21 are longer than tall. Neural spines do not exceed the height of their respective centra in the preserved cervicals and neural spine length increases proportionally faster than height. The posterior margins of the neural spines are convex overall, with a rugose, posteriorly projecting process at spine mid-height beginning at cervical four and becoming more pronounced throughout the series. *Cardiocorax mukulu* also bears a posterior projection near mid-height of the neural spine (Araújo et al., 2015a) but differs from MOR 3072 in also possessing an anteriorly projecting process.

Almost all anterior cervical ribs (3–7 and 13–21) are fused, although the sutures are clearly visible. In cervical vertebrae 8–12 however, ribs are unfused and fully separated from the centra. As is visible in field photographs, all posterior cervical ribs are also unfused and displaced. Anterior-most cervical ribs bear a dorsolaterally positioned ridge

along most of their length, resulting in a triangular cross-sectional view of ribs 4–10. Gradually, the ridge reduces its length distally so that it becomes primarily an anteroposteriorly-oriented ridge at the midlength of ribs 11–21 (Fig 8). These more posterior ribs are thickest in their proximal half and thinnest distally. Rib morphology posterior to cervical 21 is unknown. In lateral view, the preserved cervical ribs have a conspicuous distal expansion that is weakly developed anteriorly and strongly developed posteriorly beginning at cervical four, similar to those of *T. haningtoni*. In ribs 15–21, the anteroposterior length of the distal rib margin is greater than the dorsoventral length of the ribs.

Dorsal vertebrae—Interpretations of the dorsal series are based on three prepared vertebrae: two anterior dorsals located adjacent to the coracoid and one middle dorsal centrum (Fig. 9). The dorsal centra are anteroposteriorly short compared to the height and width of the centra, which are approximately equal in dimension (Table 1). The transverse processes of all three dorsals are situated more ventrally on the neural arches relative to *Hydrotherosaurus alexandrae*. The transverse processes of the anterior dorsals are inclined dorsally at 20–25 degrees from the horizontal and angled slightly posteriorly. The cross-sectional shape of the transverse processes is subcircular, with somewhat flattened ventral surfaces. The diameter of the distal articular facet of the transverse process is approximately twice the diameter mid-shaft. The articular facets for the dorsal ribs are rounded in lateral view, convex, and face posteroventrally. The preserved dorsal neural spine is approximately equal in height to its respective centrum. MOR 3072 displays a faint anteroposterior constriction along the base of the neural spines, in contrast to *Albertonectes vanderveldei*, which has none. In

lateral view, the neural spines are roughly rectangular in shape and mediolaterally thin (9.2 cm tall, 0.6 cm wide and 5.5 cm long in the best preserved spine). Other data regarding the number and morphology of dorsal vertebrae will be available once preparation of the large concretionary block is complete.

Caudal vertebrae—Five partially prepared and articulated caudal vertebrae are visible in MOR 3072, likely from the anterior portion of the tail; however, the total number of caudal vertebrae is unknown (Fig. 10). Centra have a length to width ratio of 1.56–1.30, which is much less than that of *Hydralmosaurus* and *Hydrotherosaurus* (0.6–0.8). MOR 3072 is autapomorphic in having proximal caudal vertebrae that are wider than dorsoventrally tall. Rib facets are located approximately at the mid-height of centra and are circular in outline. The chevron facets are located exclusively along the posteroventral margin of the centrum, similar to *A. vanderveldei*, and are not shared between adjacent centra as in *Hydralmosaurus serpentinus* (Welles, 1943). The location and prominent size of the chevron facets produce a sharply angled ventral centrum margin in posterior view. Two parallel, anteroposteriorly-oriented ridges are located along the ventral surface of the centrum, similar to *Hydrotherosaurus alexandrae* (Welles, 1943). One or two pairs of ventral foramina are located medial and/or lateral to the ventral ridges. All of the preserved caudal ribs are unfused with the centra. The caudal ribs are dorsoventrally flattened, bear a slight anteriorly-projecting process about mid-length, and are approximately equal in length to the width of their corresponding centra in the preserved series. A single disarticulated chevron is preserved that curves posteriorly in lateral view (Fig. 10).

Appendicular Skeleton

Coracoids—The clavicular arch, scapulae, and anterior third of the coracoids (including the glenoid fossae, anteromedial process of the coracoid and margins of the pectoral fenestrae) were lost to erosion; however, the posterior two-thirds of the coracoids were collected and the ventral surface prepared (Fig 11.) The left and right coracoids are not fused but remain in articulation with only a small area of contact ventrally along the midline, leaving a broad V-shaped gap in anterior view between each symphyseal facet (Fig. 11A). Whether this relationship between the left and right coracoids was partly or wholly present in life or simply a result of dorsoventral compression is unclear. A prominent, ventral transverse ridge extends from the approximate location of the glenoid fossa (although this is missing) toward the midline. An anteroposteriorly short, ventrally-projecting, medial process is present where the transverse ridges merge along the midline. The ventral process appears to have extended 5 centimeters from the base of the blade and was smoothly rounded before being damaged in the field. There is no evidence of a very pronounced ventral process as is seen in *Wapuskanectes betsynichollsae*. The outline of the intercoracoid vacuity is cordate and similar in shape to, but proportionally larger than, that of *Callawayasaurus colombiensis*. The posterolateral cornu extends at least as far laterally as the glenoid fossa and possibly further, based upon the placement of the left humeral head as seen in field photographs (Fig. 2), similar to *Hydrotherosaurus alexandrae*, *C. colombiensis*, and *W. betsynichollsae*. Although MOR 3072 is an adult, the coracoids do not meet posterior to the intercoracoid vacuity, as seen in *W. betsynichollsae*. The posterior margins of the coracoid blades are broadly convex in ventral view, similar to most

elamosaurids, but proportionally larger and more bulbous, rather than being fan-shaped as in *C. colombiensis*. MOR 3072 also displays a proportionally larger gap between the left and right posterior coracoid blades than that exhibited by *Libonectes morgani*.

Forelimbs—Portions of both forelimbs are preserved in MOR 3072. The left forelimb consists of preaxial portions of the distal humerus, the articulated radius and a partial intermedium. The right forelimb, which is more complete, includes the distal third of the humerus, the complete epipodial, mesopodial, and the metapodial rows as well as portions of seven proximal phalanges (Fig. 12). Humeral length is estimated at 39–41 cm long, based upon data extrapolated from field photographs of the left side. Maximum width is approximately 55% of midline length, compared to 73% in *Wapuskaneptes betsynichollsae* (Druckenmiller and Russell, 2006), 64% in *Terminonatator ponteixensis* (Sato, 2003) and 64–65% in *Futababasurus suzukii* (Sato et al., 2006). Thus, the humerus is relatively shorter and broader than other described North American elasmosaurids. Distally, the preaxial margin of the distal humerus is slightly convex; the shape of the postaxial margin is unclear due to damage. The entire distal end of the humerus is separated into two facets, a large radial facet (68% of total distal width) and a smaller ulnar facet (32%). The radial facet of MOR 3072 is proportionately much larger than that seen in the humeri of *T. ponteixensis* (56%) and *F. suzukii* (50–52%). Both facets are concave and angled at 155 degrees relative to each other.

The preaxial margin of the radius and the postaxial margin of the ulna are straight. The radius is anteroposteriorly wider than proximal-distally long (14.5 cm and

13 cm, respectively) and has a clearly defined articular facet for the radiale and intermedium. The presence of an articular facet on the proximal radius suggests the presence of a preaxial accessory ossicle, similar to that seen in *Morenosaurus stockii* (Welles, 1943). A well-formed epipodial foramen is present and less than half the length of the epipodials. The ulna is equal in proximodistal length to the radius, but it is roughly 75% the width of the radius and has well-formed facets for the intermedium, ulnare, and the proximal accessory ossicle.

Two postaxial accessory ossicles are present: the proximal, which is incomplete, lies between the epipodial and proximal mesopodial row and the distal ossicle, which is complete, lies between the proximal and distal mesopodial rows and contacts metapodial V. It is unclear if a third postaxial accessory ossicle similar to the proximal ossicle in *M. stockii* (Welles, 1943) articulated to the humerus and proximal end of the ulna. The distal accessory ossicle is smaller than metacarpal V and possesses well-defined articular surfaces for the ulnare and metacarpal V. The distal mesopodial row contains carpals 1, 2, 4, and metacarpal V, which has shifted proximally into the postaxial margin of this row. Carpal 2 articulates with the radiale and intermedium; carpal 4 articulates with both the intermedium and ulnare. The proximal margins of metacarpals II and III are bi-faceted for articulation with both mesopodial 1 and 2, and 2 and 4, respectively.

Only the proximal ends of the first row of phalanges are articulated in the right forelimb; however, more distal phalanges are visible and semi-articulated in the block containing the caudal vertebrae (Fig. 10). MOR 3072 displays an interlocking pattern between adjacent digits, unlike *F. suzukii* (Sato et al., 2006), *A. vanderveldei*, and *T.*

ponteixensis, although only the proximal phalanges are preserved in *T. ponteixensis*. All preserved phalanges are less than twice as long as wide, similar to other elasmosaurids such as *A. vanderveidei* and *F. suzukii* (Sato et al., 2006).

Ilia—Both ilia are preserved and the right is completely prepared (Fig 13). Because the pelvic girdle is largely articulated (although slightly compressed), it is possible to determine the relative position and orientation of the ilia with confidence. For orientation purposes, I refer to the sacral end of the ilium as dorsal and the acetabular end as ventral. In dorsal view, the dorsal end of the ilium is anteroposteriorly elongate and a rugosity is visible along the concave medial surface where the sacral rib facet is located. In medial view, the dorsal margin is slightly wider than the ventral margin (6.3 cm and 5.9 cm, respectively), but in anterior view the dorsal margin is approximately half the width of the ventral margin (4 cm and 8.2 cm, respectively). In lateral view, the dorsal portion of the ilium is separated from the anteriorly and laterally curving ventral half by a posteriorly projecting ‘knee’, similar to CM Zfr 159 (1994.91.1) (Hiller et al., 2014). The cross-sectional shape at the midpoint of the shaft is subtriangular with the flat surfaces facing medially and posterolaterally and a subrounded face directed anteriorly. The acetabular facet occupies roughly 70% of the ventral surface of the ilium and faces anterolaterally, while the ischial facet is approximately 30% of the ventral surface of the ilium and faces posterolaterally. The edge between the acetabular and ischial facets is a hummocky protrusion that does not extend up the shaft of the ilium, in contrast to the groove that extends between the facets and into the shaft of SGO.PV.6506 (Otero et al., 2014).

Hindlimbs—Only the proximal third of the right femur is preserved, while the left hindlimb is represented by a complete femur, the dorsomedial half of the tibia and a small fragment of the fibula. The maximum width to midline length of the left femur is 57% compared to 63% in *Terminonatator ponteixensis* (Sato, 2003) and 64-71% in *Futababasurus suzukii* (Sato et al., 2006). In preaxial view, the femur is concave dorsally and convex ventrally (Fig. 14). The femur is approximately 75% the length of the humerus. Both femora preserve a hummocky capitulum and trochanter that are constricted along the pre- and postaxial surfaces but are broadly connected along the epiphyseal surface. The trochanter faces posterodorsally, is located directly dorsal to the capitulum, and is not offset pre- or post-axially. The insertion for the adductor musculature is located ventrally along the proximal third of the diaphysis where it is deeply rugose. The cross-sectional shape of the femur at this rugosity is subcircular with a flattened ventral margin. In dorsal view, the tibial facet of the femur appears straight but is slightly concave in ventral view. The left distal propodial margin is separated into two shallow facets, a large tibial (73% of total distal length) and smaller fibular facet (27%). For comparison, the total distal length of facets on the femur of *T. ponteixensis* is 59% tibial and 41% fibular and *F. suzukii* is 48% tibial and 52% fibular. The tibial facet is more concave than the shallow fibular facet and they are angled at 150 degrees relative to each other.

The tibia is approximately 78% the width of the radius. A small articular facet, possibly for an accessory ossicle (not preserved), is located along the distal preaxial margin of the femur and continues onto the proximal margin of the tibia. The presence of preaxial accessory ossicles in the hindlimb has not been documented in any known

elasmaurids. The presence of an epipodial foramen is equivocal. The proximal margin of the tibia has a squared articular margin with the propodial, in contrast to the rounded convex margin of *T. ponteixensis*. In ventral view, the preaxial half of the tibia is depressed but this artifact is attributed to taphonomic crushing.

PHYLOGENETIC ANALYSIS

The data matrix was constructed (Supplementary Data) in Mesquite version 2.75 (build 564) (Maddison and Maddison, 2010) using a modified version of the Benson and Druckenmiller (2013) matrix with 270 unordered characters and 89 operational taxonomic units (OTUs). The matrix included all non-elasmaurid taxa of the Benson and Druckenmiller (2013) matrix, with the addition of MOR 3072 and ten additional elasmaurid OTUs, including *Albertonectes vanderveldei*, *Aristonectes quirquinensis*, *Elasmosaurus platyurus*, *Hydralmosaurus serpentinus*, *Mauisaurus haasti*, SMNK-PAL 3978 (=‘*Libonectes*’ *atlasense*), *Styxosaurus snowii*, *Terminonatator ponteixensis*, *Tuarangisaurus keyesi*, and *Zarafasaura oceanis*. *Yunguisaurus liae* is the outgroup taxon. The matrix was analyzed in TNT version 1.1 (Dec 2013 version; Goloboff et al., 2000; Goloboff et al., 2008) using the ‘Tree Fusing’ command with the minimum length designated to be found 100 times and other settings left at default. During the strict consensus calculation, branches with no possible support were collapsed.

Clade support was calculated using absolute Bremer support by searching for suboptimal trees using Tree Bisection and Reconnection (TBR)-swapping. Searching for groups not lost in suboptimal trees used the sectorial, tree-drifting, and tree fusing

algorithms with one replication each and 10 drifting cycles for constraints. Best scores were found with and without constraints for monophyly. Trees were saved and exported as a NEXUS file to be modified in Mesquite. The Bremer support tree was saved as a metafile after being previewed in TNT.

Rogue taxa were identified in Mesquite using the Taxon Instability method (Maddison and Maddison, 2010), which produces a statistic that summarizes taxon movement among a predetermined set of trees, using the difference in patristic distance between all taxon pairs across every tree in the file. The end result is a scattergram that plots all taxa with the proportion of missing data per taxon on the x-axis and instability on the y-axis.

To test tree congruence, I first reran the original Benson and Druckenmiller (2013) matrix, which was analyzed in PAUP (Swofford, 2002) to determine if TNT could produce an identical topology. The TNT 'Tree Fusing' method was used and the resulting strict consensus tree is identical to Benson and Druckenmiller (2013:Fig. 2).

The analysis of the expanded data set including MOR 3072 and additional elasmosaurids resulted in 295 Most Parsimonious Trees (MPTs) after 3,012,105,627 rearrangements with the best tree length of 1427 steps. The relationships among Elasmosauridae recovered in the strict consensus tree are shown in Figure 15 (the full tree is presented in Supplementary Data 2). In the strict consensus tree of all plesiosaurians, results were largely congruent with those of Benson and Druckenmiller (2013), differing only in the position of *Attenborosaurus conybeari*, *Thalassiodracon hawkinsii*, and *Brancaosaurus brancai*, the first two of which are also the first and seventh most unstable taxa (Supplementary Data 3). Because specimens from

Elasmosauridae were well resolved and did not appear in the top 20 most unstable taxa, I opted to not remove any rogue taxa (Supplementary Data 3).

As in the Benson and Druckenmiller (2013) analysis, Elasmosauridae was recovered as the sister group of Leptocleidia, which together define the clade Xenopsaria, consisting of all Cretaceous plesiosauroids. Early Cretaceous elasmosaurids are recovered as most basal, with the exception of Santonian-aged *Elasmosaurus platyurus*. *Futabasaurus* and *Tuarangisaurus* are successive sister taxa to all remaining elasmosaurids, which cluster into two clades (nodes 1 and 3, Fig. 15) with all derived taxa possessing a complete or mostly complete cervical series, with the exception of *Aristonectes parvidens*. Node 1 includes SMNK-PAL 3978 (= '*Libonectes' atlasense*) from the Turonian of Morocco as sister taxon to three WIB specimens and MOR 3072 as sister-taxon to Campanian elasmosaurids *Hydralmosaurus serpentinus* + *Styxosaurus snowii*. The Bearpaw Formation elasmosaurids *Terminonatator* and *Albertonectes* are recovered as sister taxa within clade 3, which also includes the WIB taxon *Libonectes morgani* and the unresolved Maastrichtian Aristonectinae + *Zarafasaura*. Unfortunately, Bremer support statistics within Elasmosauridae are not highly supported, although it should be noted the branch support is very similar to Benson and Druckenmiller (2013).

Stability of tree topology was tested by running alternate iterations in TNT. The Tree Fusing algorithm was run additionally with the five most unstable taxa removed and again with the ten most unstable rogue taxa removed. The three most unstable elasmosaurids (*Elasmosaurus platyurus*, *Wapuskanectes betsynichollsae*, and *Aristonectes parvidens*, respectively) were successively removed from additional Tree

Fusing iterations but every consensus decreased tree resolution. Alternatively, I ran the 'x-mult' algorithm in TNT that Araújo et al. (2015) used with all OTUs, which also resulted in decreased resolution.

DISCUSSION

Overall, the topology is largely congruent with current phylogenetic analyses (Benson and Druckenmiller, 2013; Araújo et al., 2015b), including the placement of Aristonectinae as an unresolved clade deeply nested within Elasmosauridae. Araújo et al. (2015a) published a cladogram with nine elasmosaurids, but Araújo et al. (2015b) only scored seven elasmosaurids in their matrix, only three of which are in both analyses. Araújo et al. (2015a) is most similar to the results recovered in this study except for their placement of *Elasmosaurus platyurus* and the basal location of *T. ponteixensis* in Elasmosauridae. The recovery of *E. platyurus* (Santonian) in the current analysis in a relatively basal position is considered suspect and may be a result of critical missing data (only 26% complete), especially from the skull, which is largely absent.

Two unequivocal synapomorphies support node 1 (Fig. 15): paired lateral foramina on the ventral surface of caudal vertebrae (191.0) and fifth metapodial shifted dorsally so half is in the metapodial row (268.1). Two equivocal synapomorphies also support node 1: squamosal posterior margin rises dorsally in lateral view (61.1) and elongate ilia (227.2). Node 2 is supported by only one unequivocal synapomorphy, phalanx proportions that are long and slender (character 270.0), and three equivocal

synapomorphies: first premaxillary tooth not significantly smaller than third (140.0), trochanter not off-set posterodorsally (253.0), and tibia larger than fibula (265.0). Node 2 is subject to scrutiny, especially since there is only one unequivocal character state (270.0: long and slender phalanx) that unites these taxa and this state has not historically been used to differentiate elasmosaurid taxa. The equivocal character state of the tibia larger than fibula (265.0), which is shared between MOR 3072 and *Hydralmosaurus*, is only present in the other two Bearpaw elasmosaurids, *Terminonatator* and *Albertonectes*. The equivocal character state of the first premaxillary tooth not significantly smaller than the third (140.0) is shared between MOR 3072 and *Styxosaurus snowii* as well as the clade Aristonectinae. It is interesting that two of the three equivocal characters that define MOR 3072 and its sister taxa are also shared amongst the elasmosaurids that come from the same formation and the derived clade of elasmosaurids that has a similar drastic reduction of cervical vertebrae.

The reduced number of cervical vertebrae in MOR 3072 is autapomorphic; MOR 3072 has the fewest number of cervical vertebrae of any complete Northern Hemisphere elasmosaur found to date. MOR 3072 is nested in a clade of long necked taxa (52-63 cervical vertebrae) and is the sister group to the WIB taxa *Styxosaurus snowii* and *Hydralmosaurus* that have approximately 20 more cervicals than MOR 3072. The tree topology suggests a reduction in the total number of cervicals in MOR 3072 compared to sister and outgroup taxa. The only elasmosaurid taxa that closely approach the reduced number of cervical vertebrae in MOR 3072 are the Maastrichtian aristonectines *Kaiwhekea katiki* and *Aristonectines quirquinensis*. Phylogenetic results indicate that aristonectines represent a lineage that independently reduced the number

of cervical vertebrae and can be distinguished from MOR 3072 by numerous other differences in skull and postcranial morphology.

Convergence in cervical vertebral morphology is also observed between MOR 3072 and aristonectines. Anterior-middle cervical vertebral dimensional relationships between dorsoventral height and anteroposterior width of MOR 3072 most closely resemble *Kaiwhekea katiki*, although the anterior-most cervicals of *K. katiki* are still proportionally larger than MOR 3072 (Cruickshank and Fordyce, 2002). Both display posteriorly overhanging neural spines, postzygapophyses that are more posterior than the neural spine margin, squared-off dorsal margins of neural spines, a faint notch along the proximal posterior margin of the rib, articular faces of the centra which are slightly concave, and a ventral notch in posterior view. The obvious difference between these two specimens is the bilobed cervical vertebrae of *K. katiki* in posterior view versus the more traditional rounded centra of MOR 3072.

The Vertebral Length Index (VLI) is a single-metric value that emphasizes the length of vertebral dimensions while still accounting for the relative height and width of centra (Brown, 1981). VLI scores are a way of comparing cervical shape and dimensions of complete or near-complete necks of specimens (O'Keefe and Hiller, 2006). VLI scores also allow researchers to compare overall neck length and morphology amongst elasmosaurids. Based on VLI scores, MOR 3072 is a non-elongate elasmosaurid (O'Keefe and Hiller, 2006). The only other non-elongate elasmosaurid from the WIB is *Libonectes morgani*. The WIB specimens *Hydralmosaurus serpentinus* and *Thalassomedon haningtoni* are not classified as either elongate or non-elongate. *Aristonectes quirquinensis* and *Hydrotherosaurus alexandrae* are Maastrichtian

elasmaurids that have a similar mean VLI score to MOR 3072 (Fig. 16). The only other Maastrichtian elasmaurids with near-complete necks are aristonectines; *Kaiwhekea katiki* with one of the lowest average VLI scores, and a juvenile specimen of *A. quirquinensis* with a mean VLI score of 54 out of only 22 cervicals measured (not included in this phylogenetic analysis). Cervical vertebral dimensions could be convergent amongst Maastrichtian elasmaurids, including MOR 3072 (Figs. 15 and 16).

Other taxa not in this phylogenetic analysis, but note-worthy because of the almost complete or complete nature of these specimen's cervical series, include a juvenile specimen of '*Aphrosaurus*' *furlongi* with a mean VLI score of 91 out of 57 cervicals measured, *Thalassomedon haningtoni* with an average VLI score of 103 from 62 cervicals measured, and SDSMT 451 with a mean VLI score of 137 from 61 cervicals measured (O'Keefe and Hiller, 2006). The authors' of descriptions of *Albertonectes* (Kubo et al., 2012), *Zarafasaura* (Lomax and Wahl, 2013), and SMNK-PAL 3978 (= '*Libonectes*' *atlasense*) (Buchy, 2005) did not include VLI scores; therefore I cannot compare them at this time. The holotypes of *A. parvidens*, *Eromangasaurus*, *Wapuskaneptes*, and the Speeton Clay plesiosaurian do not have enough cervical vertebrae preserved to calculate a mean VLI that accurately represents the cervical series.

Otero et al (2015) attempted to categorize elasmaurids into three different morphotypes based upon cervical count and VLI averages, but it should be noted that they did not conduct a phylogenetic analysis. Unfortunately, a number of elasmaurids do not fall into the three classifications of aristonectine, intermediate, or extreme long-

necked morphotypes: SMNK-PAL 3978 (= *Libonectes atlasense*) with 53 cervical vertebrae (Buchy, 2005), *Morenosaurus stocki* with 46 cervicals (Welles, 1962), *Terminonatator ponteixensis* with 51 cervical vertebrae (although incomplete neck) and an average VLI of 126 (Sato, 2003), and MOR 3072 with a maximum of 42 cervical vertebrae and an average VLI of 92.

Reduction of the number of cervical vertebrae does not necessarily translate to shorter body length; Otero et al (2014) note that despite a decrease in the number of cervical vertebrae in aristonectines, the overall body length is still near 10 m, which is close in size to the extreme long-necked specimen *Albertonectes vanderveldei* at 11.2 m (minus skull). This is very different from both *Terminonatator ponteixensis*, estimated at 7 m, and MOR 3072 at 4.5–5 m. A juvenile species of *Aristonectes quirquinensis* (SGO.PV.260) has been estimated to be 4.5 m long but only 22 cervical vertebrae were preserved (Otero and O’Gorman, 2012).

The holotype of a new elasmosaur, MOR 3072, is from the lower Maastrichtian units of the Bearpaw Formation. In terms of its stratigraphic range, MOR 3072 is nearest to *Albertonectes vanderveldei* and *Terminonatator ponteixensis*, both elasmosaurids from the Canadian Bearpaw Shale. MOR 3072 is the youngest Western Interior elasmosaurid currently described, being 2–3 million years younger than *Terminonatator* (Campanian *Baculites cuneatus*–*B. reesidei* zone) and 3–4 million years younger than *Albertonectes* (Campanian *B. compressus* zone) (Sato, 2003; Kubo et al., 2012).

It is interesting to note that both the longest (*A. vanderveldei*), and shortest (MOR 3072) neck lengths of non-aristonectine elasmosaurids in the WIS are from the same

Campanian-Maastrichtian geologic formation. MOR 3072 is the third described elasmosaurid from the Bearpaw Shale, one of few Cretaceous elasmosaurids with detailed skull and postcranial osteology available for study, and one of the smallest adult elasmosaurids yet discovered. MOR 3072 provides evidence for an even more diverse assemblage of elasmosaurids at the end of the Cretaceous than previously thought by being one of the last occurring plesiosaurs from the Western Interior and possessing an extremely short neck (in overall length and cervical count) in a clade renowned for its dramatic neck elongation.

FIGURES

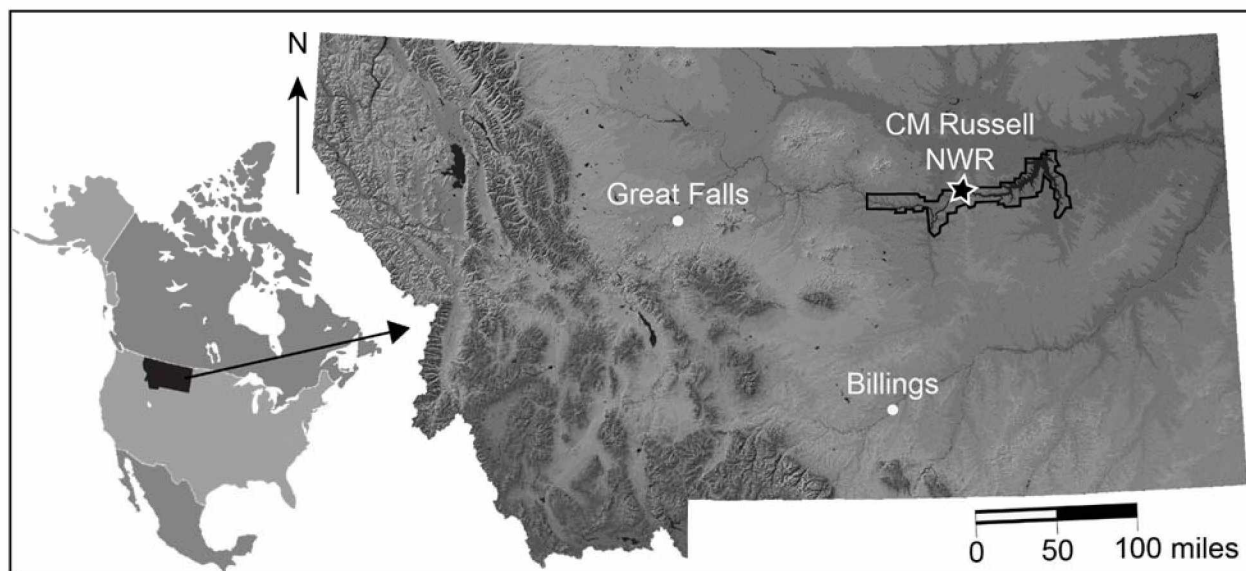


FIGURE 1. Map of locality. MOR 3072 in south Phillips County within the Charles M. Russell Wildlife Refuge (CMRWR) adjacent to the Fort Peck Reservoir, Montana, U.S.A. Outline indicates the CMRWR boundaries. [planned for page width]

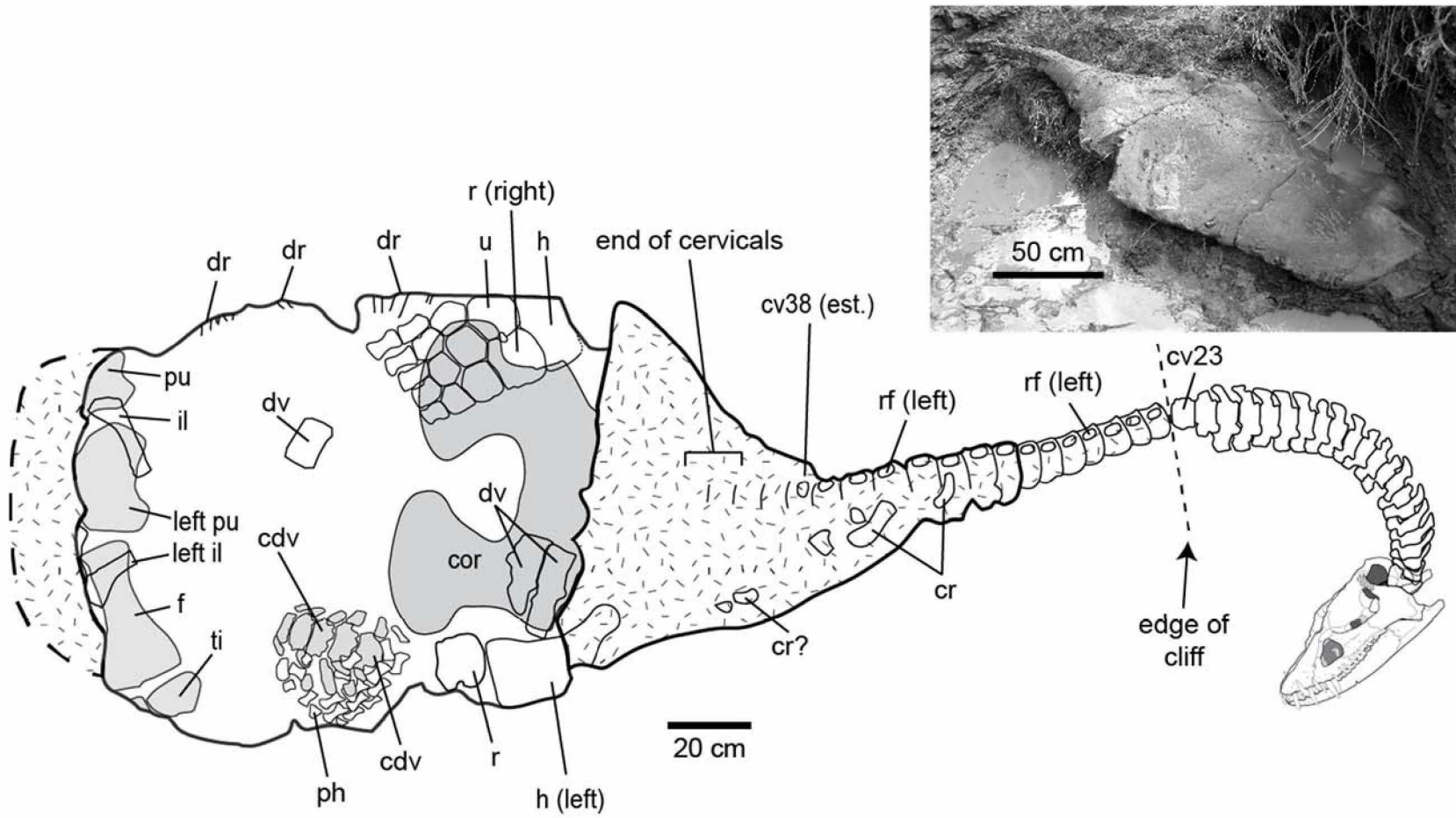


FIGURE 2. Articulated specimen with photo of MOR 3072. Photo taken by David Bradt upon discovery. **Abbreviations:** **cdv**, caudal vertebrae; **cor**, coracoid; **cr**, cervical rib; **cv#**, cervical vertebrae number; **dr**, dorsal rib; **dv**, dorsal vertebrae; **f**, femur; **h**, humerus; **il**, ilium; **ph**, phalanx; **pu**, pubis; **r**, radius; **rf**, rib facet; **ti**, tibia; **u**, ulna. [planned for page width]

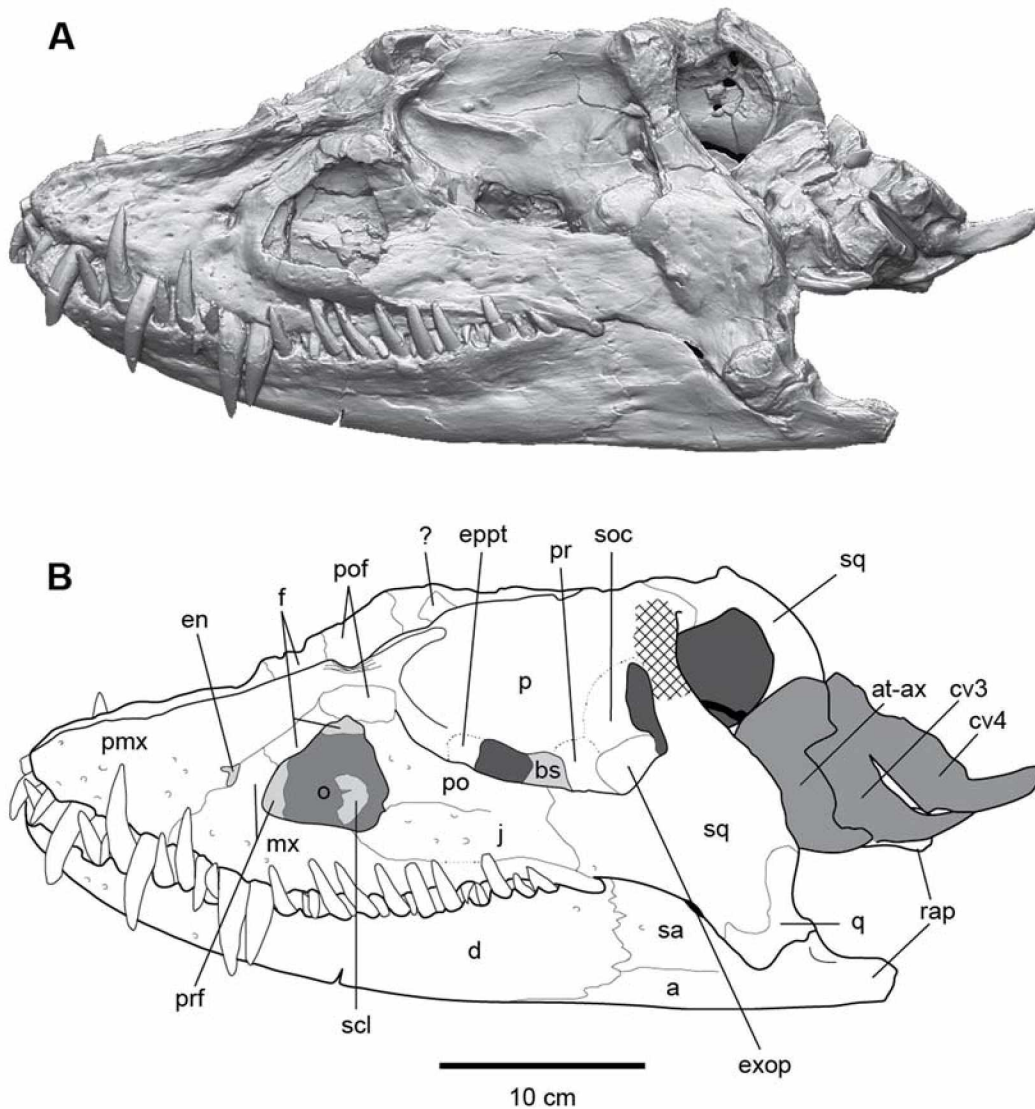


FIGURE 3. Dorsal view of skull. **A**, dorsal and left lateral scan, and **B**, interpretation of the skull of MOR 3072. Cross-hatching indicates damaged area. **Abbreviations:** **a**, angular; **at-ax**, atlas-axis; **bs**, basisphenoid; **cv#**, cervical vertebrae #; **d**, dentary; **en**, external nares; **eppt**, epipterygoid; **exop**, exoccipital-opisthotic; **f**, frontal; **j**, jugal; **mx**, maxilla; **o**, orbit; **p**, parietal; **po**, postorbital; **pof**, postfrontal; **pr**, prootic; **prf**, prefrontal; **pmx**, premaxilla; **q**, quadrate; **rap**, retroarticular process; **sa**, surangular; **scl**, scleral; **soc**, supraoccipital; **sq**, squamosal. [planned for page width]

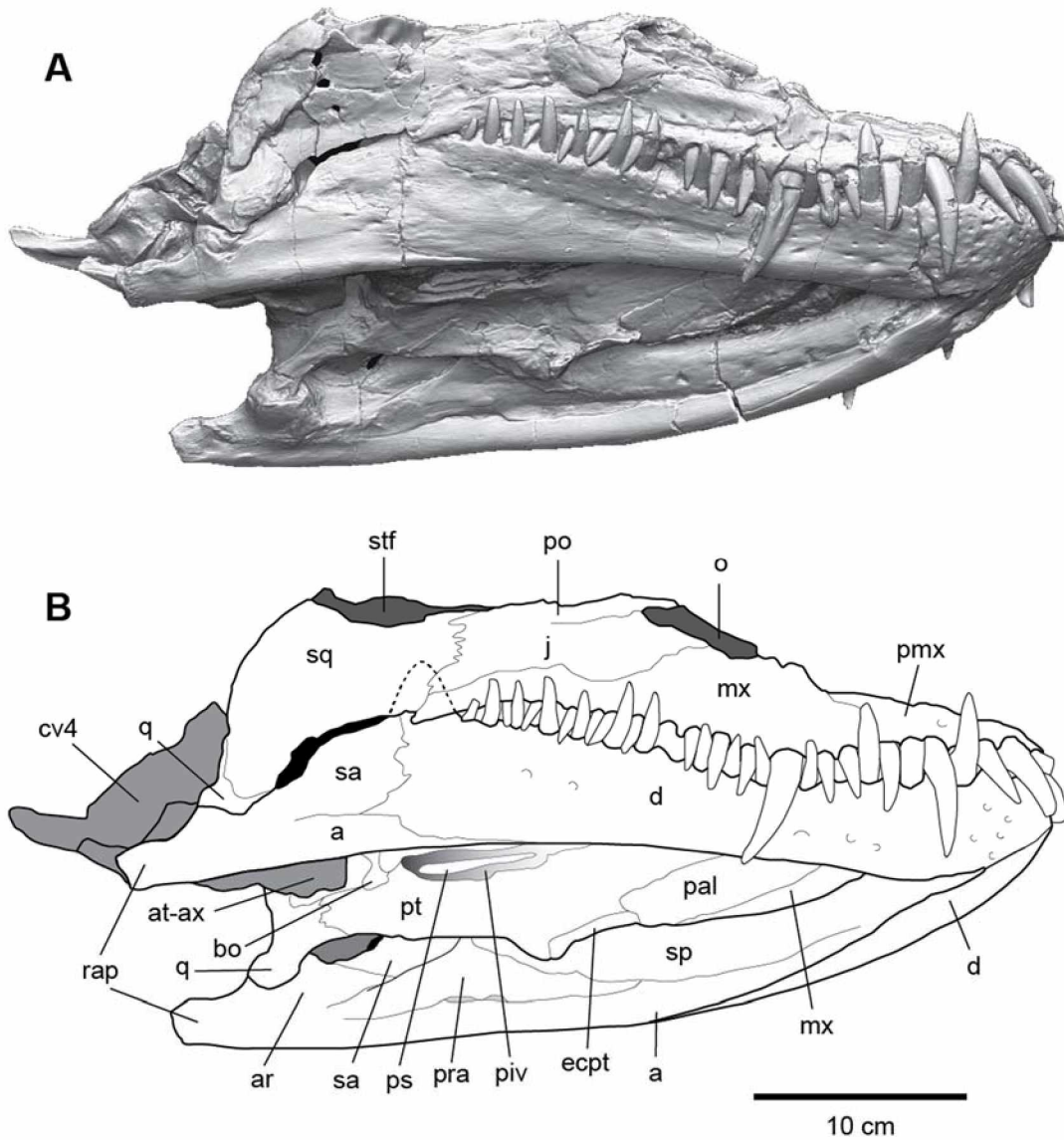


FIGURE 4. Ventral view of skull. **A**, ventral and right lateral scan, and **B**, interpretation of the skull of MOR 3072. Dashed line indicates location of coronoid process.

Abbreviations: **a**, angular; **ar**, articular; **at-ax**, atlas-axis; **bo**, basioccipital; **cv#**, cervical vertebrae #; **d**, dentary; **ecpt**, ectopterygoid; **j**, jugal; **mx**, maxilla; **o**, orbit; **pal**, palatine; **piv**, posterior interpterygoid vacuity; **pmx**, premaxilla; **po**, postorbital; **pra**, prearticular; **ps**, parasphenoid; **pt**, pterygoid; **q**, quadrate; **rap**, retroarticular process; **sa**, surangular; **sp**, splenial; **sq**, squamosal; **stf**, supratemporal fenestra. [planned for page width]

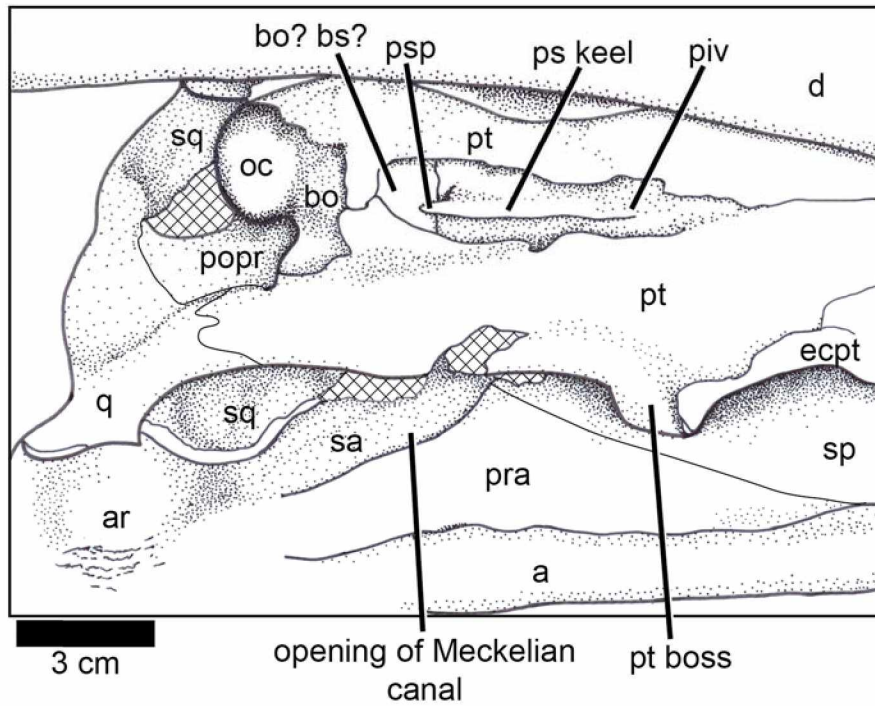
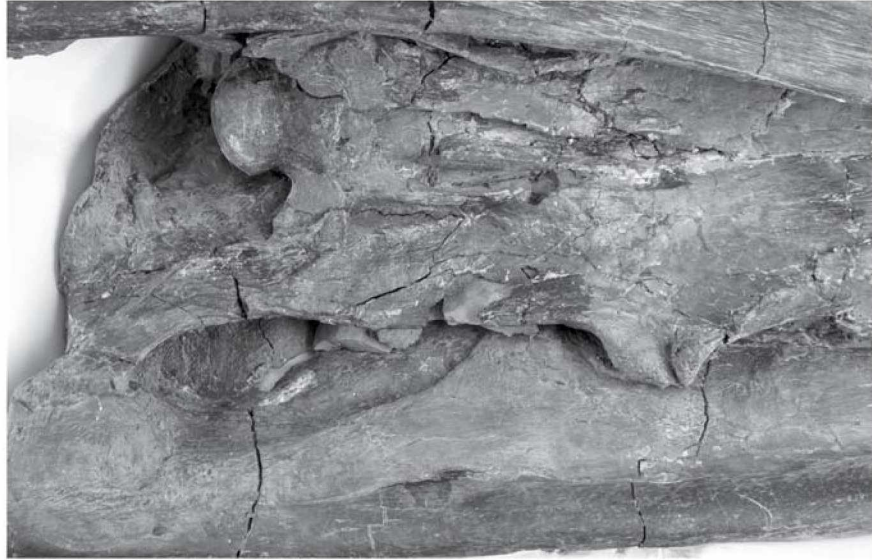


FIGURE 5. Palatal view of skull. Ventromedial view of the skull of MOR 3072.

Abbreviations: **a**, angular; **ar**, articular; **bo**, basioccipital; **bs**, basisphenoid; **d**, dentary; **oc**, occipital condyle; **piv**, posterior interpterygoid vacuity; **popr**, paraoccipital process; **pra**, prearticular; **ps keel**, parasphenoid keel; **psp**, parasphenoid process; **pt**, pterygoid; **pt boss**, pterygoid boss; **q**, quadrate; **sa**, surangular; **sp**, splenial; **sq**, squamosal.

[planned for page width]

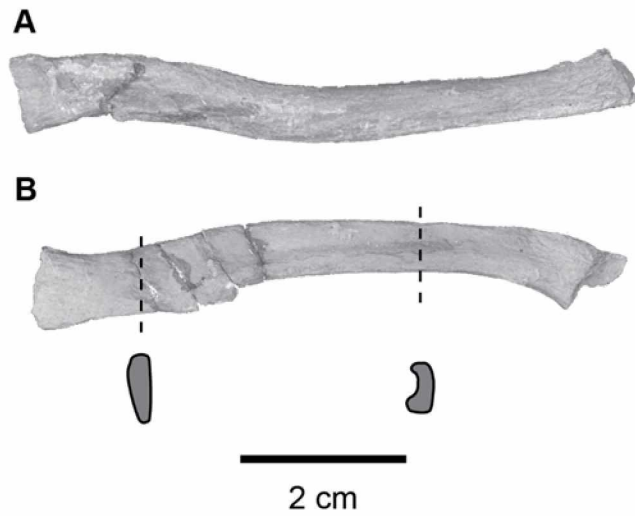


FIGURE 6. Hyoids. MOR 3072 in **A**, left and **B**, right medial view. Anterior is to the left. Cross sectional views are from anterior. [planned for column width]

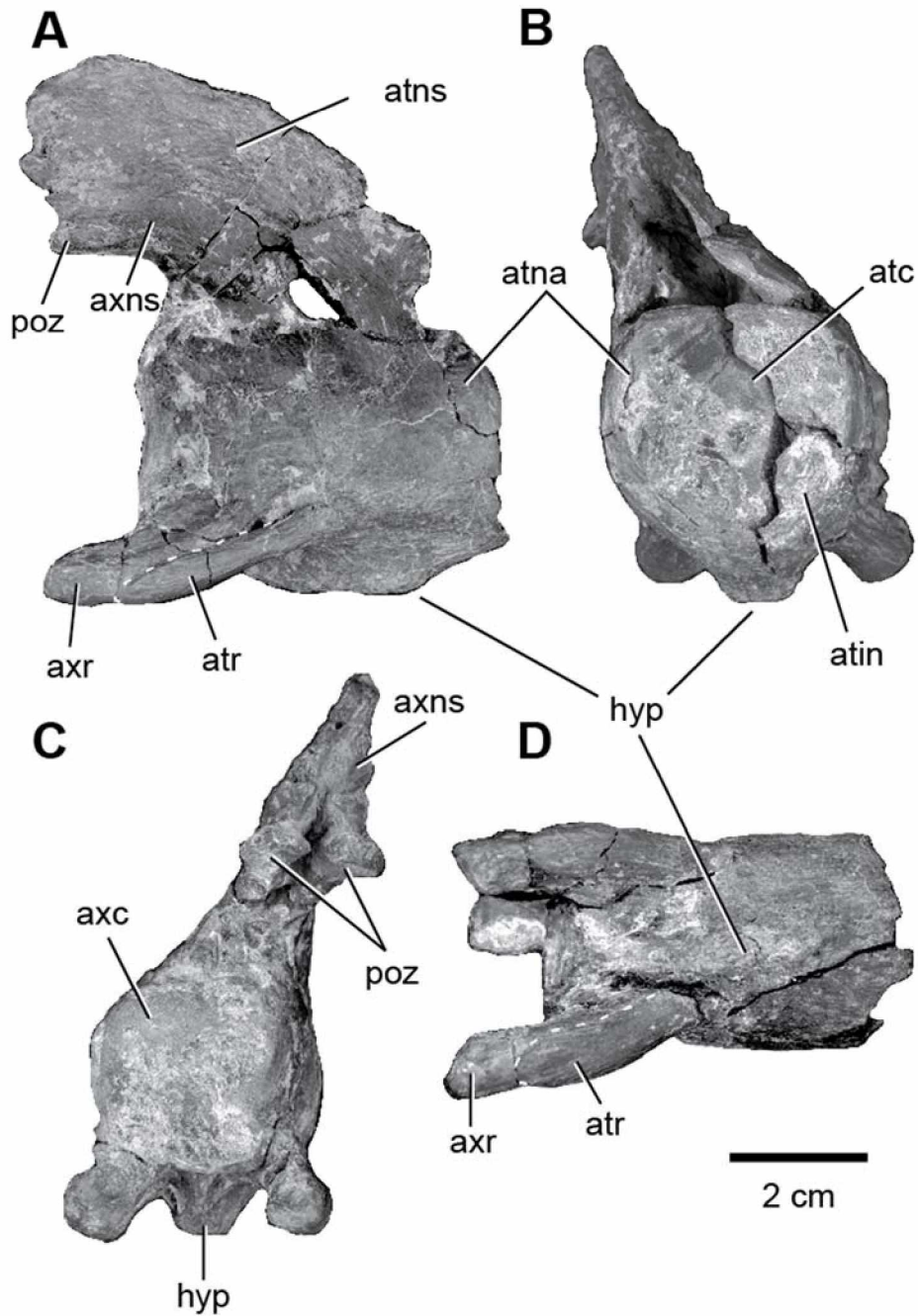


FIGURE 7. Atlas-axis. MOR 3072 in **A**, right lateral, **B**, anterior, **C**, posterior, and **D**, ventral views. **Abbreviations:** **atc**, atlantal centrum; **atin**, atlantal intercentrum; **atna**, atlantal neural arch; **atns**, atlantal neural spine; **atr**, atlantal rib; **axc**, axial centrum; **axns**, axial neural spine; **axr**, axial rib; **hyp**, hypophyseal ridge; **poz**, postzygapophysis.

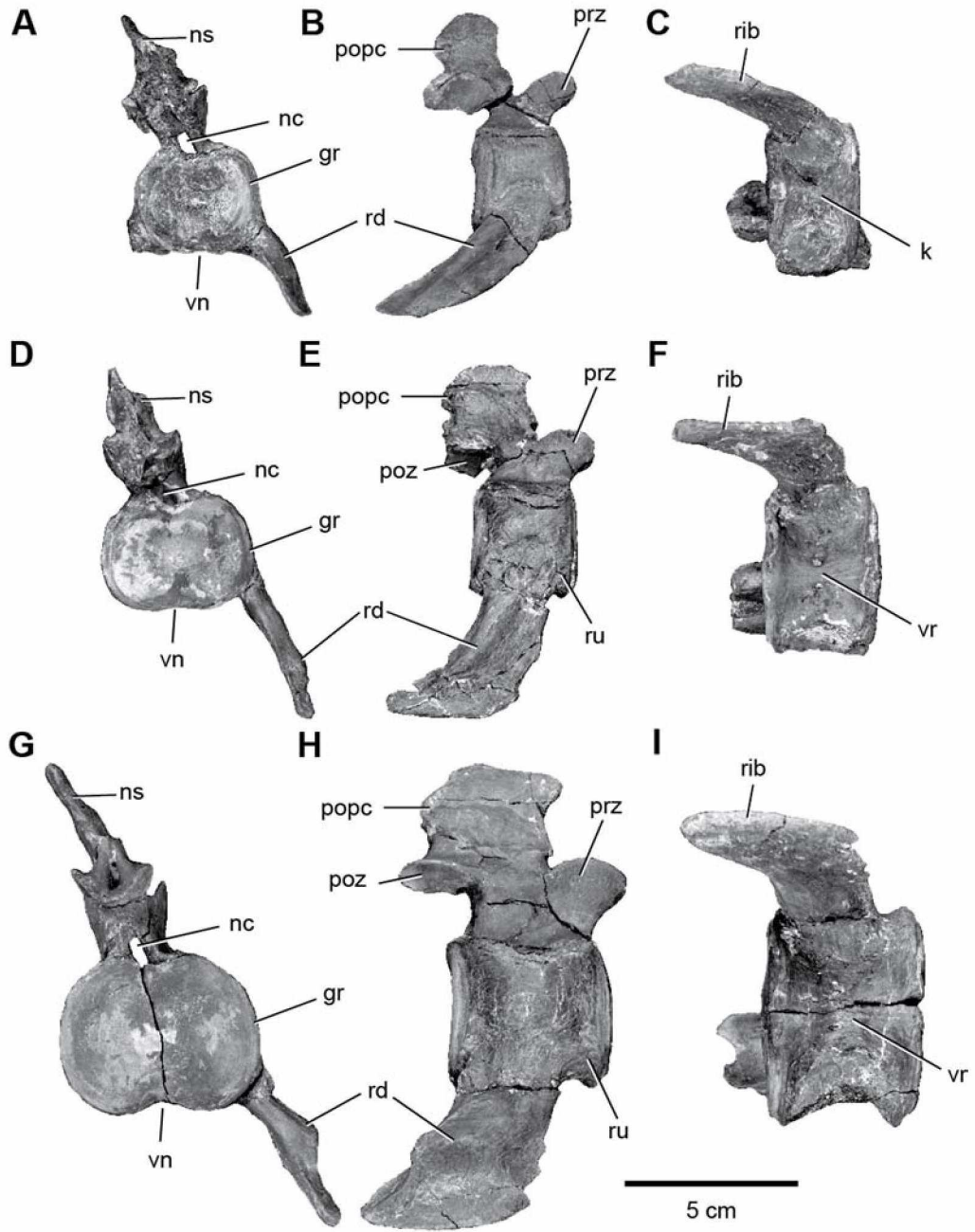


FIGURE 8. Cervical vertebrae 4, 8, and 18. **A**, Posterior, **B**, right lateral, and **C**, ventral view of cervical 4. **D**, Posterior, **E**, right lateral, and **F**, ventral view of cervical 8. **G**, Posterior, **H**, right lateral, and **I**, ventral view of cervical 18. **Abbreviations:** **gr**, groove; **nc**, neural canal; **ns**, neural spine; **popc**, posterior process; **prz**, prezygapophysis; **poz**, postzygapophysis; **rd**, ridge; **ru**, rugosity; **vn**, ventral notch. [planned for page width]

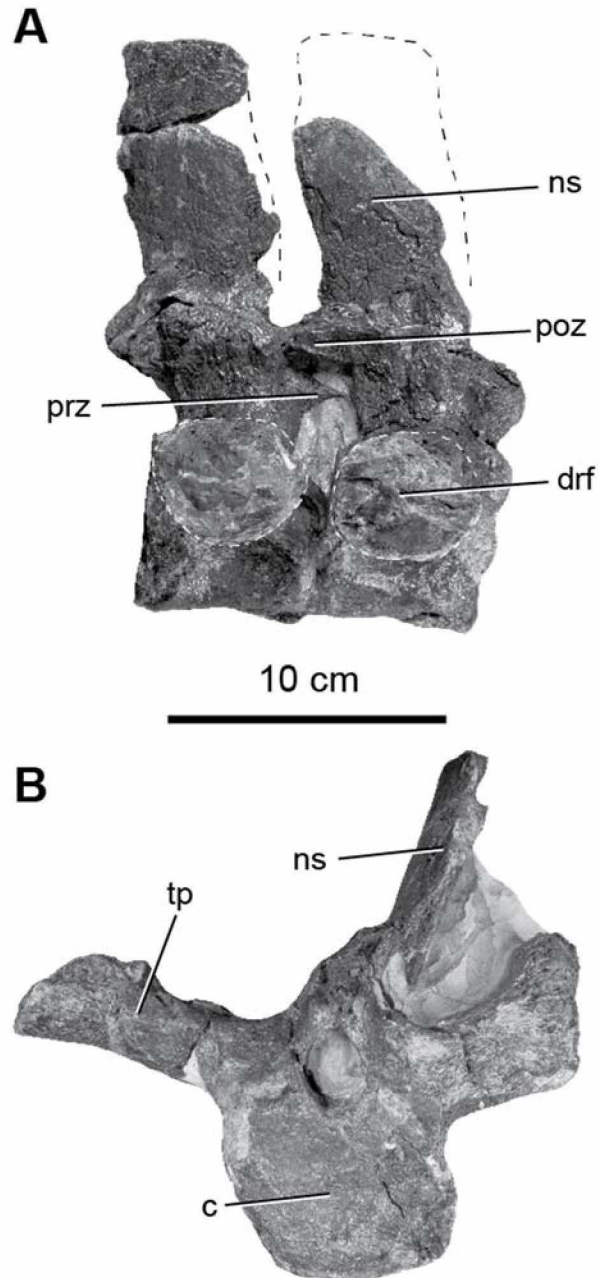


FIGURE 9. Dorsal vertebrae. MOR 3072 in **A**, lateral and **B**, anterior views. White dashed line indicates dorsal rib facet. Black dashed line indicates estimated margin of neural spines and transverse process. **Abbreviations:** **tp**, transverse process; **drf**, dorsal rib facet

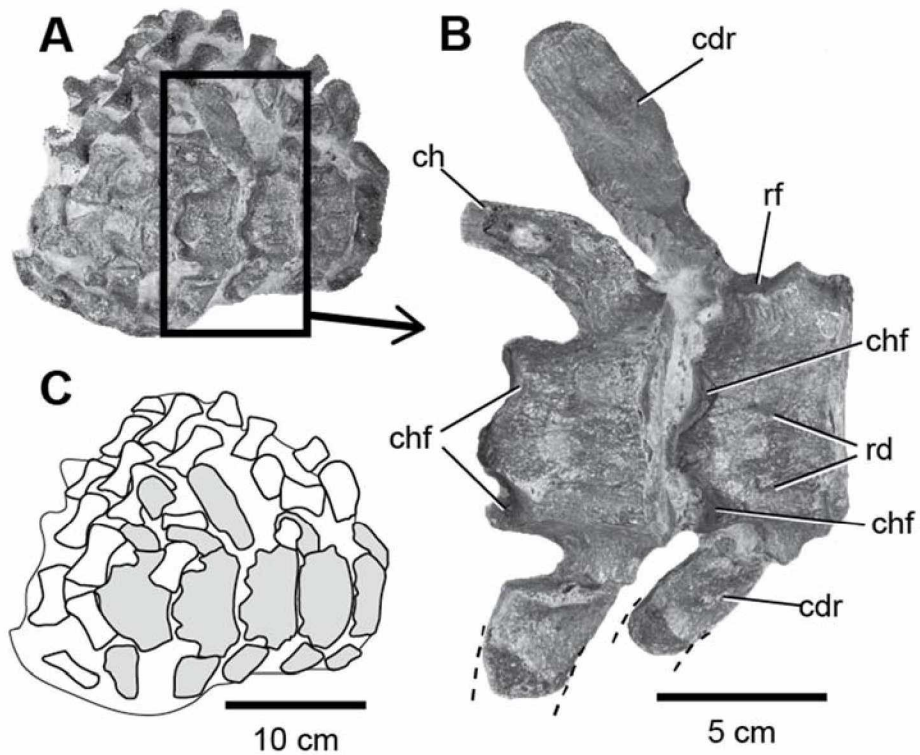


FIGURE 10. Caudal vertebrae and phalanges. Ventral view of **A**, caudal vertebrae and phalanges, **B**, close-up of two anterior caudal vertebrae, and **C**, interpretation.

Abbreviations: **cdr**, caudal rib; **ch**, chevron; **chf**, chevron facet; **rd**, ridge; **rf**, rib facet.

[planned for 2/3 page width]

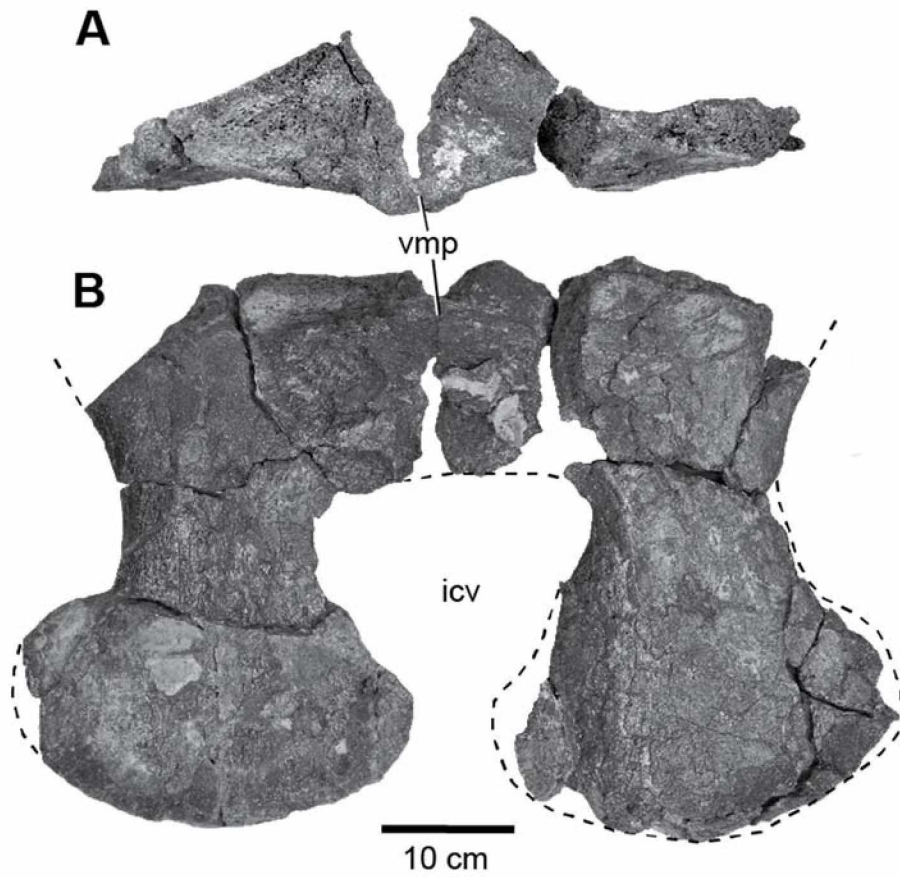


FIGURE 11. Coracoid. MOR 3072 in **A**, anterior and **B**, ventral views. **Abbreviations:**

icv, intercoracoid vacuity; **vmp**, ventromedial process. [planned for page width]

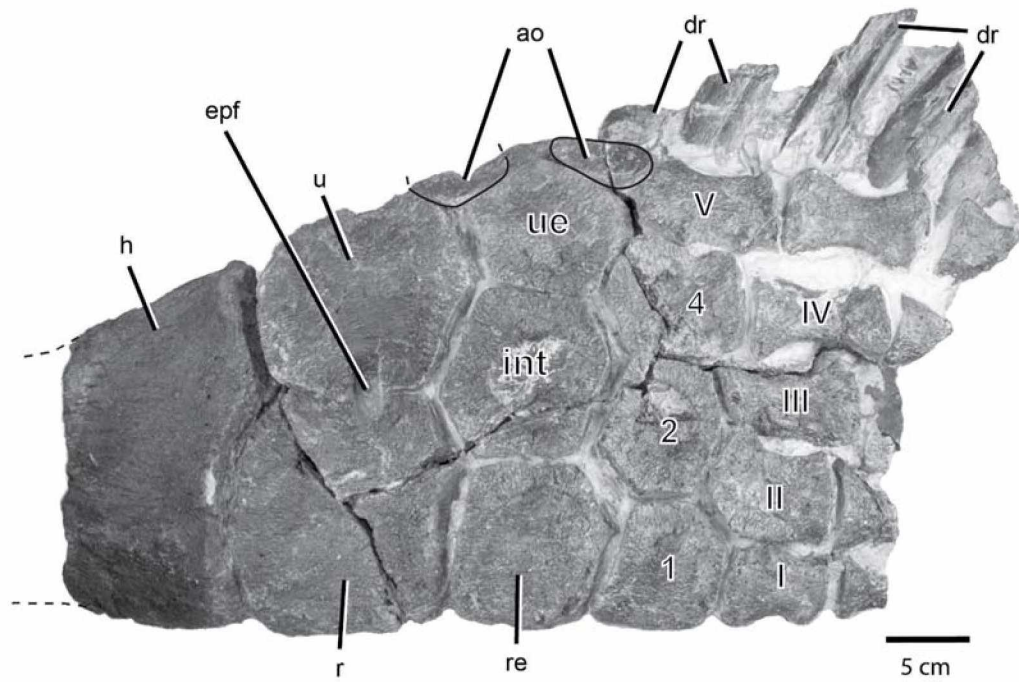


FIGURE 12. Right forelimb. Dorsal view of MOR 3072. Dashed line indicates where missing bone is expected. **Abbreviations:** **ao**, accessory ossicles; **dr**, dorsal rib; **epf**, epipodial foramen; **h**, humerus; **int**, intermedium; **r**, radius; **re**, radiale; **u**, ulna; **ue**, ulnare; **1–4**, distal carpals; **I–V**, metacarpals. [planned for page width]

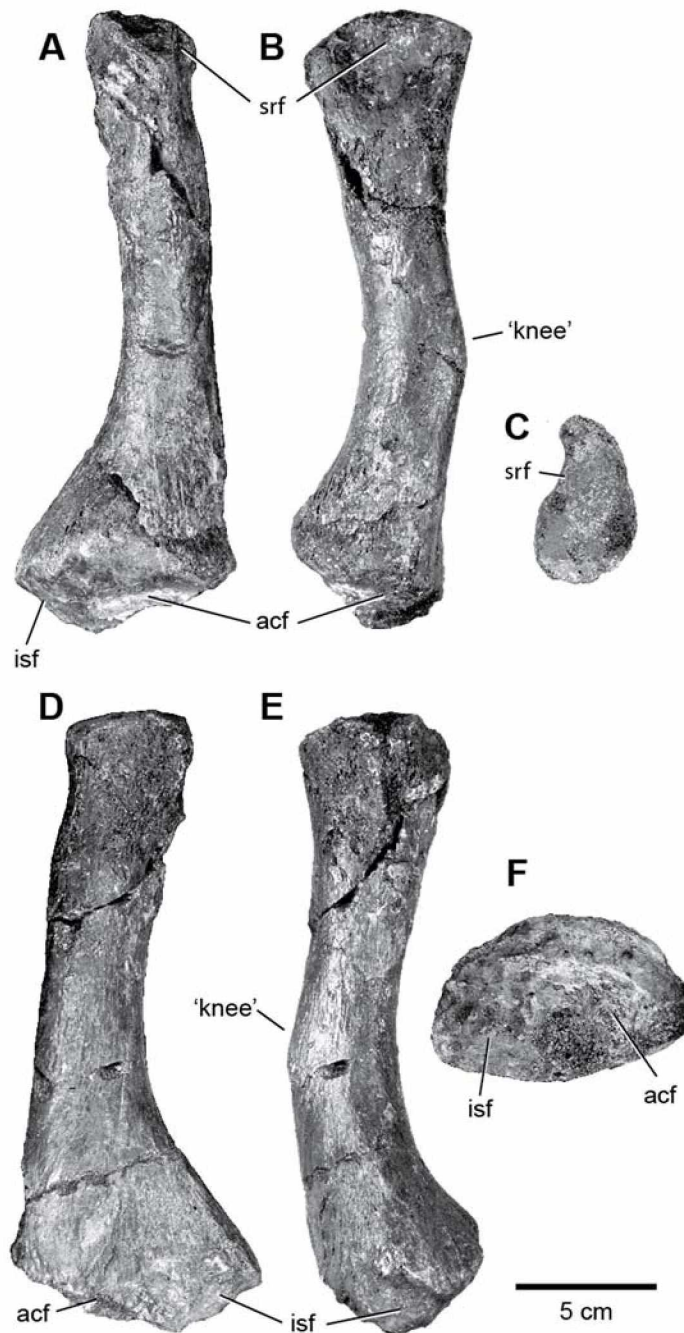


FIGURE 13. Right ilium. MOR 3072 in **A**, anterior, **B**, medial, **C**, dorsal, **D**, posterior, **E**, lateral, and **F** ventral views. For **C** and **F**, anterior is up. **Abbreviations:** **acf**, acetabular facet; **isf**, ischial facet; **srf**, sacral rib facet. [planned for page width]

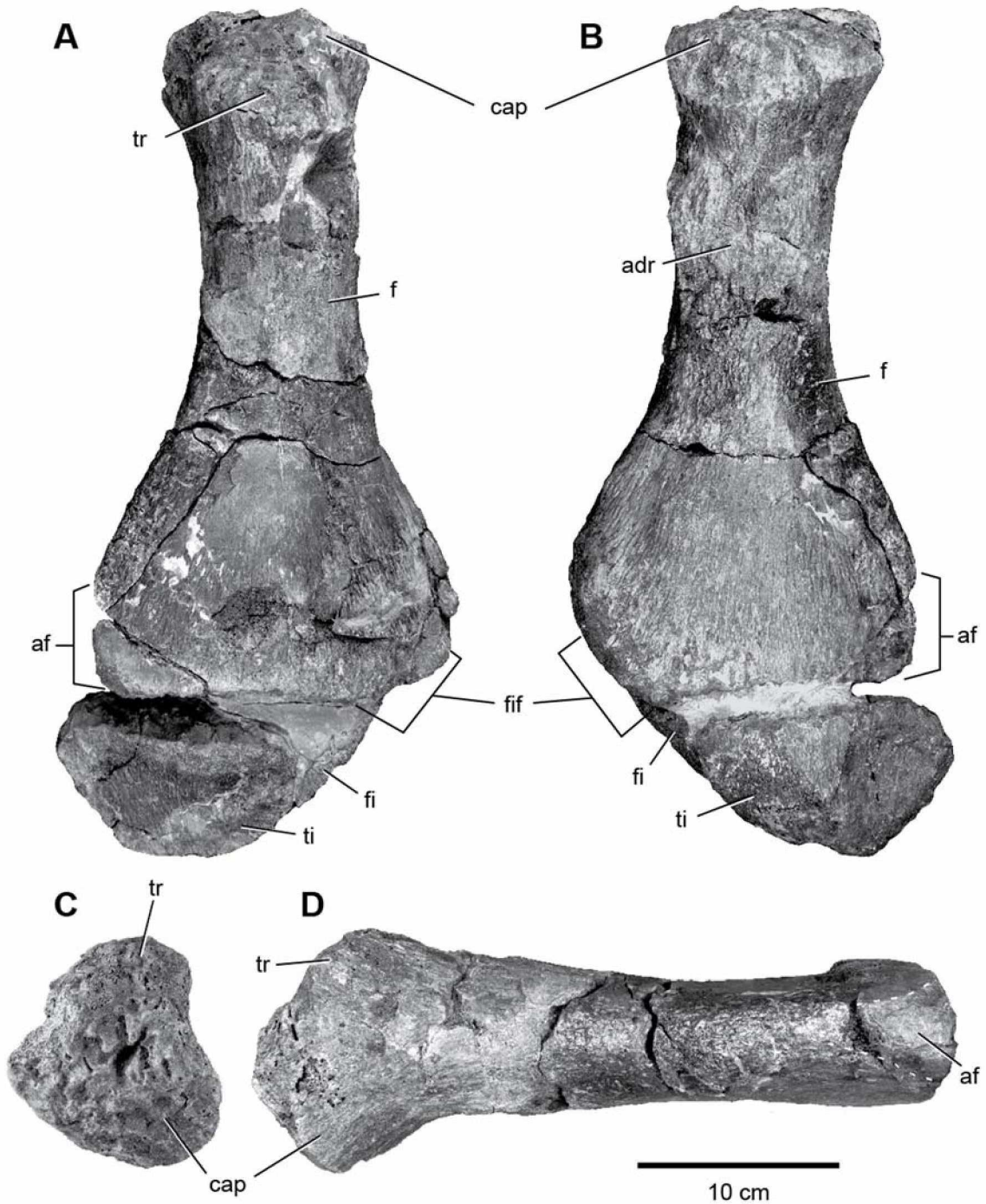


FIGURE 14. Left hindlimb. MOR 3072 in **A**, dorsal, **B**, ventral, **C**, proximal, and **D**, preaxial views. Dashed line indicates where unknown element articulates to femur.

Abbreviations: **af**, articular facet; **adr**, adductor rugosity; **cap**, capitulum; **f**, femur; **fi**, fibula; **fif**, fibula facet; **ti**, tibia; **tr**, trochanter. [planned for page width]

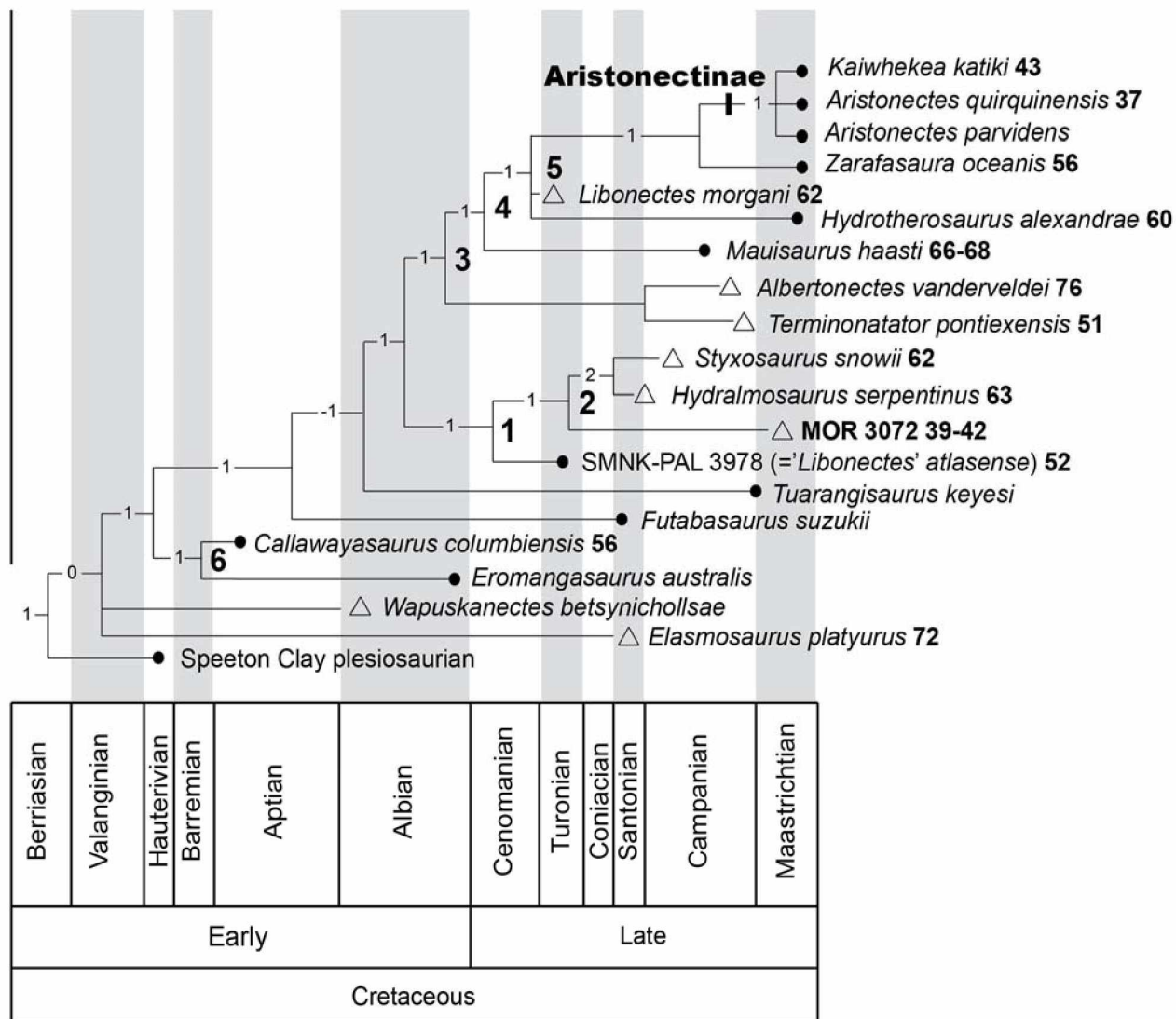


FIGURE 15. Cladogram. Stratigraphically calibrated strict consensus tree of Elasmosauridae. Numbers adjacent to nodes are Bremer support values calculated using the full taxon set. Larger number in bold are node numbers referred in text. Numbers in bold next to taxa names are cervical vertebral count. Triangles designate WIS elasmosaurids and dots designate all other localities. [planned for page width]

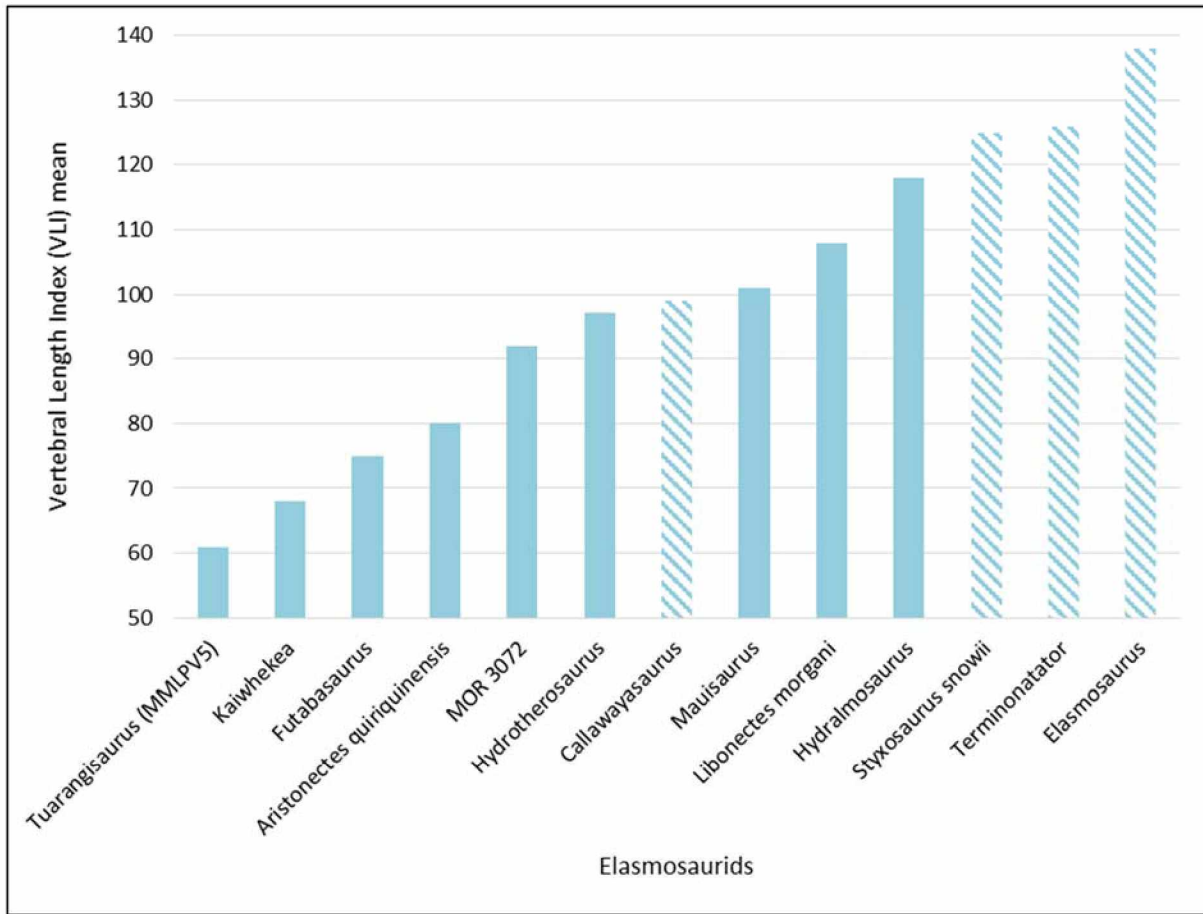


FIGURE 16. Mean VLI of 13 elasmosaurid cervical series. A mean VLI<110 is a non-elongate. Stripes indicate WIS specimens. [planned for 2/3 page width]

TABLES

TABLE 1. Measurements. Skull and postcranial material of MOR 3072.

Skull length	32.9 cm	tip of the rostrum to the posterior end of the occipital condyle
Preorbital length	10.8 cm	tip of premaxilla to anteriormost point of orbit
Dorsal vertebra Delta ventral length	6.5 cm	anteroposterior ventral midline
Dorsal vertebra Delta centrum width	8.4 cm	lateral midline on posterior articular face
Dorsal vertebra Delta centrum height	9.2 cm	dorsoventral midline on posterior articular face
Dorsal vertebra Delta total height	22.0 cm	dorsoventral midline from ventral centrum margin to dorsal neural spine margin
Dorsal vertebra Echo ventral length	6.0 cm	anteroposterior ventral midline
Dorsal vertebra Echo centrum width	7.6 cm	lateral midline on posterior articular face
Dorsal vertebra Echo centrum height	9.0 cm	dorsoventral midline on posterior articular face
Dorsal vertebra Foxtrot ventral length	7.0 cm	anteroposterior ventral midline

TABLE 1 continued

Dorsal vertebra Foxtrot centrum width	8.0 cm	lateral midline on posterior articular face
Dorsal vertebra Foxtrot centrum height	9.5 cm	dorsoventral midline on posterior articular face
Estimated humerus midline length	39-41 cm	extrapolated from field photographs
Humerus distal width	22.0 cm	widest point of distal margin
Radius length	13.2 cm	midline proxidistal length
Radius width	13.4 cm	midline lateral width
Forelimb width epipodial row	26.0 cm	including accessory ossicles
Forelimb width mesopodial row	28.5 cm	including accessory ossicles
Femur midline length	30.0 cm	proxidistal length
Femur distal width	17.0 cm	widest point of distal margin
Femur proximal width	11.0 cm	widest point of proximal margin
Coracoid width	67.0 cm	lateral width from left to right cornu
Ilium length	22.0 cm	dorsoventrally longest length

TABLE 2. Vertebral dimensions and VLI. Cervical series of MOR 3072

Cervical	VLI	L (mm)	H (mm)	W (mm)	length/height	length/width
C3	74.74	24.94	27.92	38.82	0.89	0.64
C4	80.36	26.72	28.00	38.50	0.95	0.69
C5	82.89	29.01	29.00	41.00	1.00	0.71
C6	81.71	30.03	30.50	43.00	0.98	0.70
C7	89.30	32.05	29.46	42.32	1.09	0.76
C8	88.21	32.25	29.16	43.96	1.11	0.73
C9	90.76	34.18	28.55	46.77	1.20	0.73
C10	88.66	34.74	30.39	47.98	1.14	0.72
C11	93.92	36.93	30.88	47.76	1.20	0.77
C12	95.36	38.80	30.71	50.67	1.26	0.77
C13	96.77	40.16	31.38	51.62	1.28	0.78
C14	93.60	41.51	34.11	54.59	1.22	0.76
C15	92.35	41.39	33.22	56.42	1.25	0.73
C16	93.99	42.55	34.87	55.67	1.22	0.76
C17	90.60	42.26	35.15	58.14	1.20	0.73
C18	90.84	43.12	36.01	58.93	1.20	0.73
C19	97.17	45.92	37.80	56.71	1.21	0.81
C20	95.41	45.91	39.60	56.64	1.16	0.81
C21	99.74	47.54	39.12	56.21	1.22	0.85
C22	93.63	48.03	40.22	62.38	1.19	0.77

TABLE 2 continued

C23	95.93	49.56	41.12	62.20	1.21	0.80
mean	90.76				1.15	0.75

LITERATURE CITED

- Araújo, R., and M. J. Polcyn. 2013. A biomechanical analysis of the skull and adductor chamber muscles in the Late Cretaceous plesiosaur *Libonectes*. *Palaeontologia Electronica* 16(2):1–25.
- Araújo R., M. J. Polcyn, A. S. Schulp, O. Mateus, L. L. Jacobs, A. Olímpio Gonçalves, and M. -L. Moirais. 2015a. A new elasmosaurid from the early Maastrichtian of Angola and the implications of girdle morphology on swimming style in plesiosaurs. *Netherlands Journal of Geosciences* 1–12.
- Araújo R., M. J. Polcyn, J. Lindgren, L. L. Jacobs, A. S. Schulp, O. Mateus, A. Olímpio Gonçalves, and M. -L. Moirais. 2015b. New aristonectine elasmosaurid plesiosaur specimens from the Early Maastrichtian of Angola and comments on paedomorphism in plesiosaurs. *Netherlands Journal of Geosciences* 1–16.
- Benson, R. B. J., and T. Bowdler. 2014. Anatomy of *Colymbosaurus megadeirus* (Reptilia, Plesiosauria) from the Kimmeridge Clay Formation of the U.K., and high diversity among Late Jurassic plesiosauroids. *Journal of Paleontology* 34(5):1053–1071.
- Benson, R.B.J., and P.S. Druckenmiller. 2013. Faunal turnover of marine tetrapods during the Jurassic–Cretaceous transition. *Biological Reviews* 1–23.

- Bergstresser, T. J., and W. N. Krebs. 1983. Late Cretaceous (Campanian-Maastrichtian) diatoms from the Pierre Shale, Wyoming, Colorado and Kansas. *Journal of Paleontology* 57(5):883–891.
- Blainville, H. D. de. 1835. Description de quelques espèces de reptiles de la Californie. *Nouvelles Annales du Muséum d'Histoire Naturelle, Paris* 4:233–296.
- Brown, D. S. 1981. The English Upper Jurassic Plesiosauroidea (Reptilia) and a review of the phylogeny and classification of the Plesiosauria. *Bulletin of the British Museum (Natural History) Geology Series* 35:253–344.
- Buchy, M. –C. 2005. An elasmosaur (Reptilia: Sauropterygia) from the Turonian (Upper Cretaceous) of Morocco. *Carolinea* 63:5–28.
- Carpenter, K. 1997. Comparative cranial anatomy of two North American Cretaceous plesiosaurs. *Ancient Marine Reptiles* 191–216.
- Carpenter, K. 1999. Revision of North American elasmosaurids from the Cretaceous of the Western Interior. *Paludicola* 2:148–173.
- Chatterjee S., and B. J. Small. 1989. New plesiosaurs from the Upper Cretaceous of Antarctica. *Geological Society Special Publication* 47:197–215.
- Cobban, W. A., K. C. McKinney, J. D. Obradovich, and I. Walaszczyk. 2006. USGS zonal table for the Upper Cretaceous Middle Cenomanian-Maastrichtian of the Western Interior of the United States Based on ammonites, inoceramids, and radiometric ages. U.S. Geological Survey Open-File Report 2006–1250:1–45.
- Cochran, J. K., N. H. Landman, K. K. Turekian, A. Michard, and D. P. Schrag. 2003. Paleooceanography of the Late Cretaceous (Maastrichtian) Western Interior

- Seaway of North America: evidence from Sr and O isotopes. *Palaeogeography, Palaeoclimatology, Palaeoecology* 191(1):45–64.
- Condon, S. M. 2000. Stratigraphic framework of Lower and Upper Cretaceous rocks in central and eastern Montana. *US Geological Survey* 303:236–1535.
- Cope, E. D. 1869. Extinct Batrachia, Reptilia and Aves of North America. *Transactions of the American Philosophical Society* 14:1–252.
- Cruikshank A. R. I., and R. E. Fordyce. 2002. A new marine reptile (Sauropterygia) from New Zealand: further evidence for a Late Cretaceous Austral radiation of cryptoclidid plesiosaurs. *Paleontology* 45(3):557–575.
- Druckenmiller, P. S., and A. P. Russell. 2006. A new elasmosaurid plesiosaur from the Early Cretaceous Clearwater Formation, northeastern Alberta, Canada. *Paludicola* 5(4):184–199.
- Feldmann R. M., G. A. Bishop, and T. W. Kammer. 1977. Macrurous Decapods from the Bearpaw Shale (Cretaceous: Campanian) of Northeastern Montana. *Journal of Paleontology* 51:1161–1180.
- Feldmann R. M., A. Frantescu, O. D. Frantescu, A. A. Klompaker, G. Logan, C. M. Robins, C. E. Schweitzer, and D. A. Waugh. 2012. Formation of lobster-bearing concretions in the Late Cretaceous Bearpaw Shale, Montana, United States, in a complex geochemical environment. *Palaios* 27(12):842–856.
- Gasparini, Z., N. Bardet, J. E. Martin, and M. Fernandez. 2003. The elasmosaurid plesiosaur *Aristonectes* Cabrera from the latest Cretaceous of South America and Antarctica. *Journal of Vertebrate Paleontology* 23(1):104–115.

- Goloboff, P. A., J. S. Farris, and K. C. Nixon. 2000. T.N.T.: Tree Analysis Using New Technology. Available at www.zmuc.dk/public/phylogeny.
- Goloboff, P.A., J. S. Farris, and K. C. Nixon. 2008. TNT, a free program for phylogenetic analysis. *Cladistics* 24:774–786.
- Großmann, F. 2007. The taxonomic and phylogenetic position of the Plesiosauroidea from the Lower Jurassic Posidonia Shale of south-west Germany. *Palaentology* 50(3):545–564.
- He, S., T. K. Kyser, and W. G. E. Caldwell. 2005. Paleoenvironment of the Western Interior Seaway inferred from $\delta^{18}\text{O}$ and $\delta^{13}\text{C}$ values of molluscs from the Cretaceous Bearpaw marine cyclothem. *Paleogeography, Paleoclimatology, and Paleoecology* 217:67–85.
- Hiller, N., A. A. Mannering, C. M. Jones, and A. R. I. Cruickshank. 2005. The nature of *Mauisaurus haasti* Hector, 1874 (Reptilia: Plesiosauria). *Journal of Vertebrate Paleontology* 25(3):588–601.
- Hiller, N., J. P. O’Gorman, and R. A. Otero. 2014. A new elasmosaurid plesiosaur from the lower Maastrichtian of North Canterbury, New Zealand. *Cretaceous Research* 50:318–331.
- Kauffman, E. G. 1984. Paleobiogeography and evolutionary response dynamic in the Cretaceous Western Interior Seaway of North America; pp. 273–306 in Westermann, G. E. G. (ed.), *Jurassic– Cretaceous Paleogeography of North America*. Geological Association of Canada Special Paper 27.
- Kauffman, E. G., B. B. Sageman, J. I. Kirkland, W. P. Elder, P. J. Harries, and T. Villamil. 1993. Molluscan biostratigraphy of the Cretaceous Western Interior

- Basin, North America. Geological Association of Canada Special Papers 39:397–434.
- Kear, B. P. 2005. A new elasmosaurid plesiosaur from the Lower Cretaceous of Queensland, Australia. *Journal of Vertebrate Paleontology* 25(4):792–805.
- Ketchum, H. F., and R. B. J. Benson. 2010. Global interrelationships of Plesiosauria (Reptilia, Sauropterygia) and the pivotal role of taxon sampling in determining the outcome of phylogenetic analysis. *Biological Reviews* 85:361–392.
- Kubo, T., M. T. Mitchell, and D. M. Henderson. 2012. *Albertonectes vanderveldei*, a new elasmosaur (Reptilia, Sauropterygia) from the Upper Cretaceous of Alberta. *Journal of Vertebrate Paleontology* 32(3):557–572.
- Larson, N. L., and N. H. Landman. 2007. The geological and paleontological contributions of William “Bill” A. Cobban. *The Journal of Paleontological Sciences* 7:1–46.
- Leckie, R. M., M. G. Schmidt, D. Finkelstein, and R. Yuretich. 1991. Paleooceanographic and paleoclimatic interpretations of the Mancos Shale (Upper Cretaceous), Black Mesa Basin, Arizona. *Geological Society of America Special Paper* 260:139–152.
- Lomax, D. R., and W. R. Wahl. 2013. A new specimen of the elasmosaurid plesiosaur *Zarafasaura oceanis* from the Upper Cretaceous (Maastrichtian) of Morocco. *Paludicola* 9(2):97–109.
- Maddison, W.P., and D.R. Maddison. 2010. Mesquite: a modular system for evolutionary analysis. Version 2.75. <http://mesquiteproject.org>
- O’Gorman, J. P., E. Olivero, and D. A. Cabrera. 2012. Gastroliths associated with a juvenile elasmosaur (Plesiosauria, Elasmosauridae) from the Snow Hill Island

- Formation (upper Campanian-lower Maastrichtian), Vega Island, Antarctica. *Alcheringa* 36(4):531–541.
- O’Keefe, F. R. 2001. The evolution of plesiosaur and pliosaur morphotypes in the Plesiosauria (Reptilia: Sauropterygia). *Paleobiology* 28(1):101–112.
- O’Keefe, F. R., and M. T. Carrano. 2005. Correlated trends in the evolution of the plesiosaur locomotor system. *Paleobiology* 31(4):656–675.
- O’Keefe, F. R., and N. Hiller. 2006. Morphologic and ontogenetic patterns in elasmosaur neck length, with comments on the taxonomic utility of neck length variables. *Paludicola* 5(4):206–229.
- Osborn, H. F. 1903. The reptilian subclasses Diapsida and Synapsida and the early history of the Diaptosauria. *Memoir of the American Natural History* 1:449–507.
- Otero, R. A., and J. P. O’Gorman. 2012. Identification of the first postcranial skeleton of *Aristonectes* Cabrera (Plesiosauridea, Elasmosauridae) from the upper Maastrichtian of the south-eastern Pacific, based on a bivariate graphic analysis. *Cretaceous Research* 1–4.
- Otero, R. A., S. Soto-Acuña, A. O. Vargas, and D. Rubilar-Rogers. 2014. A new postcranial skeleton of an elasmosaurid plesiosaur from the Upper Cretaceous of central Chile and reassessment of *Cimoliasaurus andium* Deecke. *Cretaceous Research* 50:318–331.
- Otero, R. A., S. Soto-Acuña, C. Salazar, and J. L. Oyarzún. 2015. New elasmosaurids (Plesiosauria, Sauropterygia) from the Late Cretaceous of the Magallanes Basin, Chilean Patagonia: evidence of a faunal turnover during the Maastrichtian along the Weddellian Biogeographic Province. 1–42.

- Owen, R. 1860. On the orders of fossil and Recent Reptilia, and their distribution in time. Report of the British Association for the Advancement of Science 29:153–166.
- Palamarczuk S., and N. H. Landman. 2011. Dinoflagellate cysts from the upper Campanian Pierre Shale and Bearpaw shale of the U.S. Western Interior. Rocky Mountain Geology 46(2):137–164.
- Sachs, S. 2005. Redescription of *Elasmosaurus platyurus* Cope 1868 (Plesiosauria: Elasmosauridae) from the Upper Cretaceous (lower Campanian) of Kansas, USA. Paludicola 5:92–106.
- Sato, T. 2002. *Terminonatator ponteixensis*, a new elasmosaur (Reptilia; Sauropterygia) from the Upper Cretaceous of Saskatchewan. PhD Thesis, University of Calgary 1–412.
- Sato, T. 2003. *Terminonatator ponteixensis*, a new elasmosaur (Reptilia; Sauropterygia) from the Upper Cretaceous of Saskatchewan. Journal of Vertebrate Paleontology 23:89–103.
- Sato, T., Y. Hasegawa, and M. Manabe. 2006. A new elasmosaurid plesiosaur from the Upper Cretaceous of Fukushima, Japan. Paleontology 49(3):467–484.
- Swofford, D. 2002. PAUP*. Phylogenetic Analysis Using Parsimony (* and Other Methods). Version 4.0b10. Sinauer Associates, Sunderland.
- Tokaryk, T. T. 1993. A plioplatecarpine mosasaur from the Bearpaw shale (Upper Cretaceous) of Saskatchewan, Canada. Modern Geology 18:503–509.

- Tourtlot, H. A. 1962. Preliminary investigation of the geologic setting and chemical composition of the Pierre Shale Great Plains region. Geological Survey Professional Paper 390:69–72.
- Vincent, P., N. Bardet, X. P. Suberbiola, B. Bouya, M. Amaghazaz, and S. Meslouh. 2011. *Zarafasauria oceanis*, a new elasmosaurid (Reptilia: Sauropterygia) from the Maastrichtian Phosphates of Morocco and the palaeobiogeography of latest Cretaceous plesiosaurs. *Gondwana Research* 19:1062–1073.
- Welles, S. P. 1943. Elasmosaurid plesiosaurs, with description of new material from California and Colorado. *University of California Memoirs* 13:125–254.
- Welles, S.P. 1952. A Review of the North American Cretaceous Elasmosaurs. *University of California Publications in Geological Sciences* 29:47–143.
- Welles, S. P. 1962. A new species of elasmosaur from the Aptian of Colombia and a review of Cretaceous plesiosaurs. *University of California Publications in Geological Sciences, University of California Berkeley* 44 (1):1–96.
- Wiffen, J., and W. L. Moisley. 1986. Late Cretaceous reptiles (Families Elasmosauridae and Pliosauridae) from the Mangahouanga Stream, North Island, New Zealand. *New Zealand Journal of Geology and Geophysics* 29(2):205–252.

OTHER MATERIALS

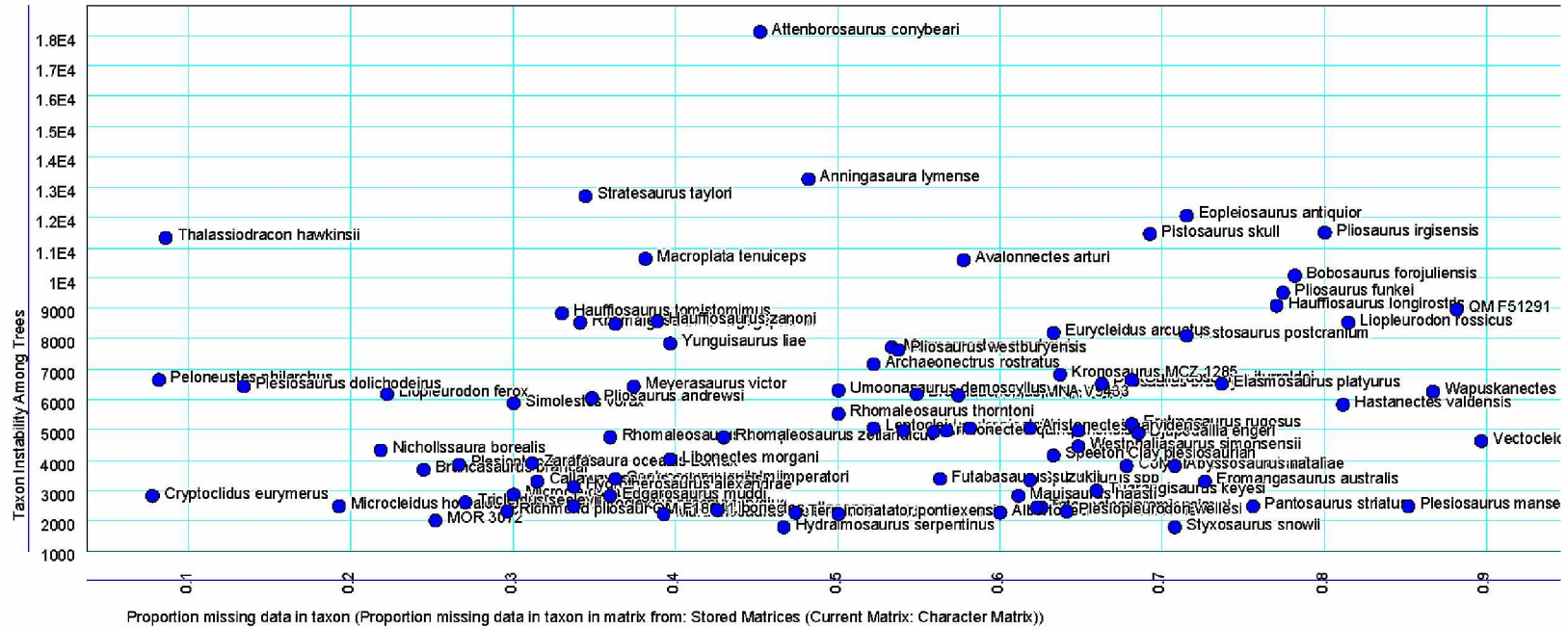
O. M. 1. Character matrix scores of MOR 3072

00001000110100201020020021?0000?00?0000100010000?320211111001110
010???201??1???1002111001?1?0000?122?0300???2011001101010100012?
01101001103021101001?02410111??3?02210111?101?0?11??1110????0101
10??????????????1?00???1?????10121021???101??00?0??03{01}011122?02
?101??101?001110

O. M. 2. Strict Consensus tree



O. M. 3. Taxon Instability scattergram



GENERAL CONCLUSION

Herein I describe a new elasmosaurid taxon from the Lower Maastrichtian Bearpaw Formation near Fort Peck, Montana, U.S.A. The specimen (MOR 3072) includes an obliquely flattened skull, the anterior 23 cervical vertebrae, the majority of the axial skeleton, a fragmented pectoral girdle, a partial pelvic girdle, gastralia, and some limb elements. It is one of the stratigraphically youngest occurring plesiosaurians from the Western Interior Seaway (WIS) of North America, one of a few Cretaceous elasmosaurids with detailed skull and postcranial osteology available for study, and the third described elasmosaurid from the Bearpaw Shale.

MOR 3072 represents a new taxon based on the following autapomorphies: a chordate bilobed external naris; a squared-off posteroventral margin of maxilla; a maxilla-squamosal contact; a deep anteroposterior oriented cleft in articular posterior to glenoid; 39–42 cervical vertebrae; proximal caudal vertebrae that are wider than dorsoventrally tall; and small facets for hindlimb preaxial accessory ossicles. MOR 3072 can further be diagnosed on the following unique character combinations: a relatively short rostrum, with rostral index of 33; the absence of a mandibular keel; a dorsoventrally-oriented premaxilla-maxilla suture; postfrontal participation in both the orbital and temporal margins; a postorbital that extends half the length of the supratemporal fenestra ventral margin; a pineal slit level with postorbital bar; a coronoid process made of the dentary only; a weakly developed medial pterygoid processes that does not obscure the basisphenoid/basioccipital; an anteriorly inclined ventral plate of the basioccipital; the absence of a lateral longitudinal ridge of the cervical vertebrae;

lateral expansion of the intercoracoid vacuity; and a dorsal expansion of the ilium twice the anteroposterior width of the midshaft.

I also conducted a new cladistic analysis of Elasmosauridae to place this new specimen in phylogenetic context. The phylogenetic matrix used for this study was modified from Benson and Druckenmiller (2013) by adding 11 new elasmosaurid OTUs, including MOR 3072. The phylogenetic analysis recovered MOR 3072 as the sister taxon to the WIS species *Hydralmosaurus serpentinus* + *Styxosaurus snowii*. Both the outgroup and sister taxa of MOR 3072 have approximately 10–20 more cervical vertebrae than MOR 3072, as well as proportionately longer vertebral centra, indicating the evolution of a markedly shorter neck in one lineage of Western Interior elasmosaurids, currently represented only by MOR 3072. The results of the phylogenetic analysis also indicate that MOR 3072 evolved a reduced neck length independently of Aristonectinae, another clade of Maastrichtian elasmosaurids known from the southern hemisphere. It is interesting to note that MOR 3072—having the shortest neck length of any non-aristonectine elasmosaurid—was recovered from the same formation as *Albertonectes*, which has the greatest number of cervical vertebrae (76) of any vertebrate known.

While resolution within Elasmosauridae is improved as a result of this study, more work is needed. Researchers often disagree about how to score specimens within morphologically-based phylogenetic matrices, which is a potential problem with the current phylogenetic analysis. Future work needed to remedy this problem includes clarifying the language of characters, developing a standard for each character score option, inviting more researchers that specialize in working with plesiosaurians to review

the characters and character scores, adding new characters, and including every taxon ever described as an OTU in the matrix.

Because MOR 3072 is not fully prepared, there is likely important information about this specimen yet to be discovered. Perhaps gastroliths and stomach contents within the cavity of the trunk are preserved that can shed light on dietary habits of elasmosaurids. The preservation of a fetus within the trunk of MOR 3072 remains a possibility since researchers cannot differentiate male from female marine reptiles (excluding specimens with preserved embryos).

MOR 3072 provides evidence for an even more diverse assemblage of elasmosaurids at the end of the Cretaceous than previously thought by being one of the last occurring plesiosaurs from the Western Interior and possessing an extremely short neck in a clade renowned for its dramatic neck elongation. Only by finding, preparing, describing, and scoring more elasmosaurid specimens for phylogenetic analysis will authors be able to better resolve the relationships amongst these astounding creatures of the Mesozoic seas. Future work needed concerning MOR 3072 should begin with the preparation of all remaining elements of the fossil, continue the search for microinvertebrates, and finally reassemble the disarticulated bones.

Finally, future work needed to bring about better resolution and understanding of Elasmosauridae includes further studies of SDSMT 451 (= '*Styxosaurus' pembertoni*) (Welles, 1949; Carpenter, 1999), SMNK-PAL 3978 (= '*Libonectes' atlasense*) (Buchy, 2005), *Zarafasaura oceanis* (Vincent et al., 2011; Lomax and Wahl, 2013), *Albertonectes vanderveldei* (Kubo et al., 2012), and *Morenosaurus stocki* (Welles, 1943; Welles, 1962). SDSMT 451 was originally named '*Alzadasaurus' pembertoni* by S. P.

Welles and later renamed by K. Carpenter. SDSMT 451 needs to be scored, possibly redescribed, and included in future phylogenetic analyses to determine accurate evolutionary relationships. SMNK-PAL 3978 was included in the genus *Libonectes* simply because it was from a geologic formation that was deposited the same time as the formation that held *Libonectes morgani*. An accurate geological age for specimens is important, but it should not be the sole reason for inclusion in an established genus. SMNK-PAL 3978 should be scored and included in future phylogenetic analyses. *Zarafasaura oceanis* and *Albertonectes vanderveldei* both have complete published descriptions but need to be scored for phylogenetic analysis and measured for Vertebral Length Index. *Morenosaurus stocki* and an associated juvenile specimen with a complete neck appear to have been forgotten by researchers. A more detailed description of these two specimens should be published along with VLI data from the juvenile, scored, and included in future analyses. While including juvenile specimens in published cladograms is not good scientific practice, they should be run in preliminary phylogenetic analyses for a clearer idea of just how much ontogeny changes results. In this mindset, '*Aphrosaurus*' *furlong* (Welles, 1943) should also be scored for future analyses.

LITERATURE CITED

Benson, R.B.J., and P.S. Druckenmiller. 2013. Faunal turnover of marine tetrapods during the Jurassic–Cretaceous transition. *Biological Reviews* 1–23.

- Buchy, M. –C. 2005. An elasmosaur (Reptilia: Sauropterygia) from the Turonian (Upper Cretaceous) of Morocco. *Carolinea* 63:5–28.
- Carpenter, K. 1999. Revision of North American elasmosaurids from the Cretaceous of the western interior. *Paludicola* 2:148–173.
- Kubo, T., M. T. Mitchell, and D. M. Henderson. 2012. *Albertonectes vanderveidei*, a new elasmosaur (Reptilia, Sauropterygia) from the Upper Cretaceous of Alberta. *Journal of Vertebrate Paleontology* 32(3):557–572.
- Lomax, D. R., and W. R. Wahl. 2013. A new specimen of the elasmosaurid plesiosaur *Zarafasaura oceanis* from the Upper Cretaceous (Maastrichtian) of Morocco. *Paludicola* 9(2):97–109.
- Vincent, P., N. Bardet, X. P. Suberbiola, B. Bouya, M. Amaghazaz, and S. Meslouh. 2011. *Zarafasaura oceanis*, a new elasmosaurid (Reptilia: Sauropterygia) from the Maastrichtian Phosphates of Morocco and the palaeobiogeography of latest Cretaceous plesiosaurs. *Gondwana Research* 19:1062–1073.
- Welles, S. P. 1943. Elasmosaurid plesiosaurs, with description of new material from California and Colorado. *University of California Memoirs* 13:125–254.
- Welles, S. P. 1949. A new elasmosaur from the Eagle Ford Shale of Texas: Systematic description. *University Press, Southern Methodist University* 1:1–28.
- Welles, S. P. 1962. A new species of elasmosaur from the Aptian of Colombia and a review of Cretaceous plesiosaurs. *University of California Publications in Geological Sciences, University of California Berkeley* 44 (1):1–96.

APPENDIX

7/1/2015

Gmail - Re: Written approval needed



Danielle Serratos <silvaraancalima@gmail.com>

Re: Written approval needed

1 message

Roger Benson <roger.benson@earth.ox.ac.uk>

Wed, Jul 1, 2015 at 12:03 AM

To: Danielle Serratos <djdavis4@alaska.edu>, Patrick Druckenmiller <psdruckenmiller@alaska.edu>

Hi Danielle,

I grant you my written approval to be a co-author on the manuscript for JVP!
Before then, I'm happy to comment on things or provide information/analyses if you need them.

Roger

On 01/07/2015 01:45, Danielle Serratos wrote:

Dr. Benson,

As per the thesis guidelines at UAF, I need your written approval via email that you will be a co-author on the manuscript we will submit to the Journal of Vertebrate Paleontology.

Thanks in advance for your time,

Danielle

--

Danielle J. Serratos

Masters candidate

Department of Geology and Geophysics,

University of Alaska Fairbanks

University of Alaska Museum of the North

Museum 010

djdavis4@alaska.edu

907-888-8449

--

Dr Roger Benson

Associate Professor - Palaeobiology

Department of Earth Sciences

<https://mail.google.com/mail/u/0/?ui=2&ik=c70ae2726&view=pt&earch=inbox&th=14e48a433386d3d5&siml=14e48a433386d3d5>

1/2

Filename: thesis_postgradoffice
Directory: C:\Users\Danielle\Documents
Template: C:\Users\Danielle\AppData\Roaming\Microsoft\Templates\Normal.dot

m

Title:
Subject:
Author: Danielle Serratos
Keywords:
Comments:
Creation Date: 7/27/2015 5:39:00 PM
Change Number: 21
Last Saved On: 7/27/2015 8:27:00 PM
Last Saved By: Danielle Serratos
Total Editing Time: 154 Minutes
Last Printed On: 7/27/2015 8:32:00 PM

As of Last Complete Printing

Number of Pages: 92
Number of Words: 17,467 (approx.)
Number of Characters: 99,563 (approx.)